5-2024

Improving Static Cold Storage Life of the Human Heart before Transplant

Juan Sebastian Rodriguez Paez
Florida Institute of Technology, jrodriguezpa2022@my.fit.edu

Improving Static Cold Storage Life of the Human Heart before Transplant

by

Juan Sebastian Rodriguez Paez

Bachelor of Science
Department of Chemical Engineering
Universidad de los Andes
2021

Bachelor of Science
Department of Physics
Universidad de los Andes
2022

A thesis
submitted to the College of Engineering and Science
at Florida Institute of Technology
in partial fulfillment of the requirements
for the degree of

Master of Science
in
Chemical Engineering

Melbourne, Florida
May, 2024

We the undersigned committee
hereby approve the attached thesis

Improving Static Cold Storage Life of the Human Heart before Transplant by Juan

Sebastian Rodriguez Paez

Venkat Keshav Chivukula, Ph.D.
Assistant Professor
Biomedical Engineering and Science
Major Advisor

Darshan G. Pahinkar, Ph.D.
Assistant Professor
Mechanical and Civil Engineering

Manolis M. Tomadakis, Ph.D.
Professor
Chemistry and Chemical Engineering

Jessica Smeltz, Ph.D.
Associate Professor and Department Head
Chemistry and Chemical Engineering

Abstract

Title:

Improving Static Cold Storage Life of the Human Heart before Transplant

Author:

Juan Sebastian Rodriguez Paez

Major Advisor:

Venkat Keshav Chivukula, Ph.D.

Organ storage and transportation are critical steps for the success of organ transplantation. Static cold storage (SCS) of hearts for heart transplantation (HTx) remains the standard approach. However, SCS may involve damage to the tissue resulting from extended hypothermic preservation, potentially affecting organ viability. Moreover, the temperature distribution on and within the heart is unknown during heart transplantation. Therefore, there is an interest to study different stages of the heart transplantation process towards determining the 3D temperature distribution on and within the heart. There could be a possibility of having a hypothermic injury in different parts of the heart due to the temperatures that are being used currently in specific parts of the heart transplantation process such as SCS icebox storage and transport. The heart transplantation process was divided into four stages: (i) when the heart is cooled within the donor via cardioplegia. (ii) when it is extracted from the donor and checked outside the body. (iii) when it is stored and transported via SCS Icebox,

(iv) when it is checked after removal and (v) when it is implanted within the recipient. To determine the 4D (3D + time) temperature distribution for each of the above stages, we utilize a custom-developed heat transfer and computational fluid dynamic simulation of the heart using COMSOL Multiphysics. The transient Bioheat transfer equation was solved using time-dependent simulations on an anatomically accurate 3D model of the heart with empirically obtained thermal properties for the cardiac muscle and surrounding tissues. Stage 1 was modelled using transient conduction by the cardioplegia fluid flow for several initial temperature conditions. For the second stage of the process, the heart simulation was performed by using the equilibrium temperature reached in the first stage as an initial condition. Stage 3 was modelled for several hours of transport using transient conduction within the icebox. Stage 2 and 4 take into account a external heat transfer resistance in comparison to the other stages. The data obtained was compared to clinical experimental data in order to obtain a quantitative analysis of the simulations as well as validation of the models.

Table of Contents

List of Figures

Acknowledgements

Mainly, I want to thank my family for their constant support and their ability to give me the strength to reach this moment. On the other hand, I want to thank my friends at the University and my fraternity brothers with whom we spent pleasant moments and constant study, which allowed me to get to know them and know the quality of people they are. I would like to thank Dr. Venkat Keshav Chivukula, Ph.D., and my co-advisor Dr Pahinkar, Ph.D. because of their support throughout this project. I would like to thank Ms Marivi Walker, Ms. Kawanda Rembert, and all the people who allowed me to contribute to this school with my knowledge and work. Also, thank each of the teachers and companions from my high school and the university Universidad de los Andes in which I obtained my Bachelors in Chemical Engineering and Physics allowing me to have the skills required for this project. All the people I have met have allowed me to love Engineering, Chemistry and Physics. I thank Florida Tech University for each of the lessons and moments special ones that will last in memory. Finally, with the support of each of the people that I have known in my learning process and with the memory of those teachers and family members who are no longer among us, I present my thesis thinking about them and remembering them forever.

Dedication

Dedicated to my father, my mother and my sister. Your constant support allowed me to advance in my career with responsibility, perseverance and discipline.

Chapter 1

Introduction

The introduction to this project report involves the state of the art for heart transplants explaining the experimental procedures as well as the conditions why these transplants have been carefully conducted. Also, it discusses the significance and innovation of this project explaining the project's objectives and the relevance for this study.

Heart transplantation remains the gold standard treatment for end-stage heart failure, offering a potential lifeline to patients with severe cardiac dysfunction. Over the past few decades, significant advancements in surgical techniques, immunosuppressive therapies, and organ preservation methods have enhanced the outcomes and expanded the pool of eligible candidates for heart transplantation. Recent research in this field has focused on refining these techniques to improve graft survival, minimize rejection risks, and enhance patient quality of life. One notable area of advancement is the utilization of ex vivo organ perfusion systems. These systems enable the assessment, preservation, and even reconditioning of donor hearts outside the body before transplantation, thus potentially expanding the donor pool and improving post-transplant outcomes. Research performed in the current decade demonstrated the efficacy of nor-

mothermic ex vivo heart perfusion in improving donor heart function and viability, leading to enhanced transplant outcomes [1].

Furthermore, the development of novel immunosuppressive strategies has been pivotal in reducing rejection rates and improving long-term graft survival. Recent studies have explored the use of tailored immunosuppression regimens based on individualized risk assessment and immune monitoring, as highlighted, which underscored the importance of personalized approaches in optimizing immunosuppressive therapy post-heart transplantation [9]. In addition to surgical and pharmacological innovations, emerging technologies such as gene editing hold promise for addressing key challenges in heart transplantation, including organ shortage and rejection. Research demonstrated the feasibility of CRISPR-Cas9-mediated gene editing to mitigate rejection responses and enhance the compatibility of donor hearts, opening new avenues for precision medicine in cardiac transplantation [13]. Despite these advancements, challenges such as organ scarcity, infection risks, and long-term graft complications persist, necessitating continued research efforts to further refine heart transplant techniques and outcomes. This review aims to provide an overview of the most recent research findings and innovations in heart transplantation, highlighting their implications for clinical practice and future directions in the field.

Heart failure is a condition that impairs the left ventricle's functionality, affecting around 63 million people worldwide [14][26] [27]. Nowadays, the treatment that is used for heart failure is a heart transplant. However, heart transplants have the risk of disparity between the donor hearts and patients that are on the waiting list for the transplant to take place [10]. It has been reported that around 40% of patients who are on the waiting list never receive a transplant. In addition to this, an unused organs

percentage exists due to the limitation of the strategies to carry out the heart transplant procedures [24] [8]. Now, to achieve heart preservation, static cold storage (SCS) is one of the strategies that is currently performed as well as ex-situ heart perfusion [25]. SCS is a method that involves cooling the heart to slow metabolic processes [20]. Figure 1.1 shows the three-bag technique, a standard method for static cold storage where the organ is suspended in a bag of a cold storage solution. But, particularly, these two bags are surrounded by two additional bags with saline and afterwards, placed into a cooler with ice (ice-box approach) [21]. This particular combination is shown in the schematic figure of figure 1.1. Nevertheless, this method has a particular problem and it is that cold storage creates cold injuries and tissue denaturation due to uneven cooling and also achieving freezing conditions of tissue. Furthermore, in this process, there are no temperature sensors which means that the temperature distribution within the heart is unknown [22]. The organ temperature is neither monitored nor the temperature distribution involving the heart geometry or shape [18]. This means that the process itself is uncertain and once a transplant is carried out, the time is limited to at least 4 hours approximately so that the organ can be used [6].

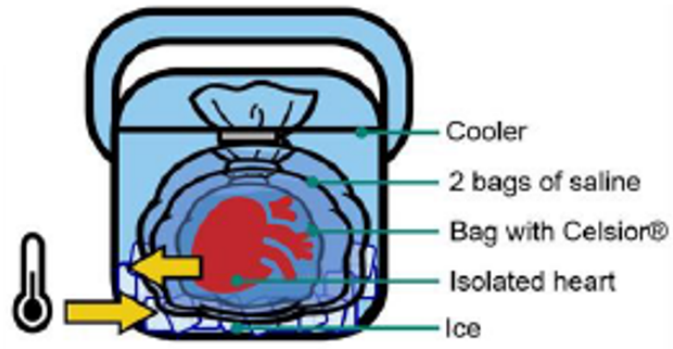

Figure 1.1: Traditional ice box approach for the static cold storage (SCS) technique. The schematic shows the suspension of the organ whose solution temperature can be controlled, but the organ temperature is not monitored.

Static cold storage (SCS) has been the traditional method for preserving donor

hearts since the inception of heart transplantation. This technique involves flushing the heart with a cold preservation solution, typically University of Wisconsin (UW) or Celsior solution, and storing it in a cold environment (typically 4^oC) to slow metabolic processes and reduce ischemic injury during transport. While SCS remains widely utilized due to its simplicity and cost-effectiveness, its limitations, including ischemia-reperfusion injury and limited preservation times, have spurred the exploration of alternative preservation methods. Ex vivo perfusion systems have emerged as a promising alternative to SCS, offering the potential to mitigate ischemia-reperfusion injury, assess organ viability, and even recondition marginal donor hearts prior to transplantation. Normothermic ex vivo heart perfusion, in particular, involves perfusing the donor heart with warm, oxygenated blood or a perfusion solution at physiological temperatures, thereby maintaining metabolic activity and preserving organ function. Current research demonstrated the superiority of normothermic ex vivo heart perfusion over SCS in preserving donor heart function and improving transplant outcomes, paving the way for its integration into clinical practice [1].

Moreover, hypothermic machine perfusion (HMP) has gained traction as an intermediate preservation method between SCS and normothermic perfusion. HMP involves perfusing the donor heart with a cold, oxygenated solution under controlled pressures, offering superior preservation compared to SCS while avoiding the complexities associated with normothermic perfusion. Recent studies have shown the efficacy of HMP in reducing ischemic injury and improving graft function, underscoring its potential as a bridge between conventional and advanced preservation techniques. In addition to advancements in organ preservation, refinements in immunosuppressive therapies have played a crucial role in optimizing transplant outcomes. Tailored immunosuppression regimens, informed by individualized risk assessment and immune monitoring,

have demonstrated superior efficacy and safety compared to traditional one-size-fits-all approaches [13]. By minimizing rejection risks while minimizing adverse effects, personalized immunosuppression holds promise for enhancing long-term graft survival and patient well-being. Despite these advancements, challenges such as organ shortage, infection risks, and long-term complications remain pertinent in the field of heart transplantation. Continued research efforts aimed at refining preservation techniques, optimizing immunosuppressive protocols, and exploring innovative approaches such as gene editing are imperative to address these challenges and further improve transplant outcomes.

1.1 Significance and innovation

The significance and innovation of this project are based on the surprising fact that studies on the internal temperature of isolated hearts have not been performed yet. The temperature distribution of the heart is also unknown as well as the effect of external conditions on the heart [21]. Particularly, these external conditions are of greater magnitude in SCS techniques [22]. This means that the proposal scope addresses the lack of knowledge in the heat transfer process and characteristics of isolated hearts. This would be addressed by heart transfer modeling including heat transfer modeling conditions. The thermal analysis will create the first database of 4D temperature distributions of isolated hearts in static cold storage processes. This collected database can determine a thermally optimal procurement technique for the heart transplant process and preservation techniques. In-silico approaches to the system will allow a parametric analysis that traditional experimentation techniques could not achieve. The simulation of the system will use a heat transfer model simulating the phenomena of cold preservation to determine the transient temperature of each region of the heart to

obtain a high-fidelity heat map of a specific heart geometry.

1.2 Objectives

The main objective of this proposal is to improve the preservation techniques for hearts that are used for heart transplant processes. This could be achieved by quantifying the heat transfer characteristics of donor hearts during transport conditions to the recipient. As it has been reported, the temperature within the heart tissue is highly influenced by thermal, physical, and hemodynamic parameters of the heart, the geometry, and its surrounding environment. For instance, the temperatures that are involved and materials, which means changes in physical properties and therefore, in the transport phenomena taking place in the geometry studied. The questions that will be answered are the following:

- How does the initial temperature of the heart influence its cooling during storage and transport?
- What is the transient temperature distribution in the heart during the traditional ice-box approach?
- What are the biological consequences of the different storage conditions and the temperatures reached during the processes?

1.3 Relevance

The proposed research is unique and the topic has not been explored with the approach proposed. Despite the critical nature of the heart transplantation processes and the need that exists in the field, there is a huge knowledge gap in assessing the health

of the organ during transport as well as the conditions that are needed to preserve its biological condition and functionality. This proposal can create the first heart thermal transplant database that quantifies the temperature distribution within the heart during procurement and organ transport. The main measure of success will be obtaining 4D transient temperature gradients and distributions during different stages of the heart transplant process. Particularly, these results will show the temperature changes experienced to have a better understanding of the biological implications of the process and the activity inside the heart, which is currently unknown.

Chapter 2

Materials and Methods

2.1 Materials

The materials involved in performing the heat transfer simulations are Autodesk Inventor to perform initial stage CAD models of simple geometries to assess basic performance. Additionally, other Autodesk tools are used to preprocess STL files of real geometries and more complex geometries such as heart STL anatomical data files. For instance, some of these important characteristics are 3D view, clapping, cutting, and additional features included in CAD modules. The simulation tool COMSOL Multiphysics is an important material since this software is used for performing the time-dependent 3D model simulations with the heat transfer in the solids module including initial conditions and boundary conditions. On the other hand, COMSOL can perform heat transfer simulations coupled with computational fluid dynamics simulations. COMSOL includes predetermined mesh methods for complex geometries that need to be addressed with a mesh independence study so that accurate results can be achieved without big computational processing times. Moreover, COMSOL includes a geometry module that is important to include to mesh and process complex geometries. The

reports that are going to be generated by COMSOL are the temperature distribution, the isothermal contours evolution, and surface plots to determine the time and the equilibrium temperatures in each of the stages of the transplantation process that are going to be explained in the Methods section.

2.2 Methods

The primary objective of this study was to leverage computational simulations to optimize temperature conditions that are suitable for heart transplant processes. The simulations were designed to explore the effects of various initial conditions and boundary conditions on temperature profiles within the organ. Particularly, there were different conditions evaluated for the cardioplegia stage as well as times that each stage of the process took. The results provided by the simulations results allowed us to suggest an optimal experimental setup so that the heart does not reach critical biological temperatures that could compromise biological functionalities. The first stage of the process refers to a cardioplegia cool-down process in which the heart is cooled down from body temperature to a certain temperature depending on the time required. The second stage of the process refers to the storage of the heart in a bag which includes a fluid solution in it. This bag is paced over ice which means there are conduction and a transient conduction modeled using an external heat transfer resistance approximated by a heat transfer coefficient of a $2.2\,mm$ layer of air. Afterward, the heart undergoes a stronger cool-down process because the bag is placed in an ice box for approximately 6 hours. Finally, the fourth and the fifth stages take place similarly to the first and the second but refer to a heat process in which the bag and the heart are removed from the icebox and heated up to be received by the recipient. Figure 2.1 and 2.2 shows a sketch of the stages involved in each simulation combination.

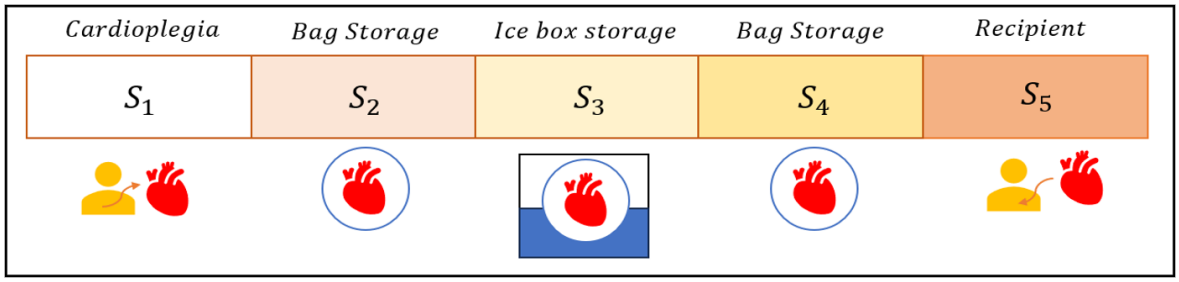

Figure 2.1: Experimental stages involved in the heart transplant process which were simulated in the conduction simulations. The second and the fourth stages do not include unsteady-state conduction effects.

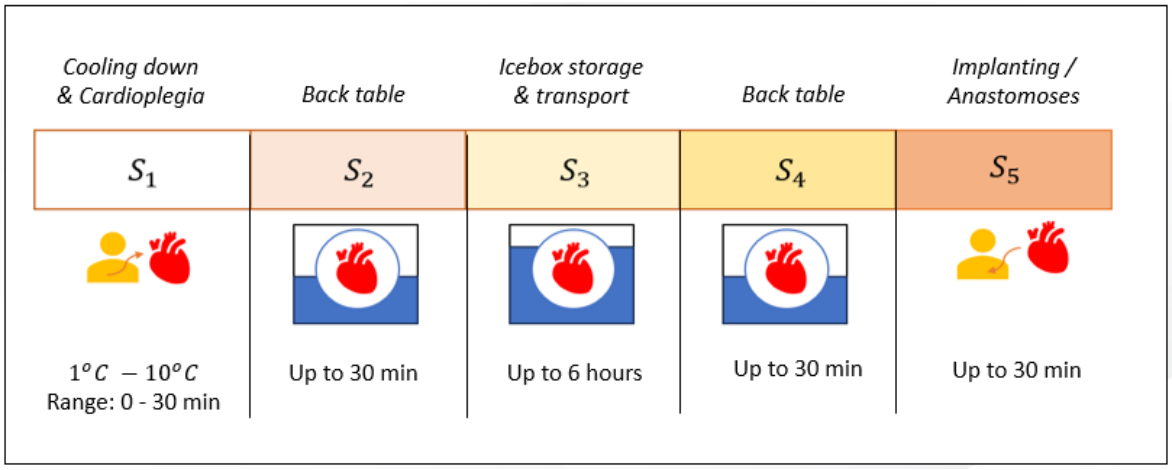

Figure 2.2: Experimental stages involved in the heart transplant process which were simulated in the conduction and unsteady-state conduction simulations. The second and fourth stages include unsteady-state conduction conditions.

2.3 Software and model development

The professional software employed was COMSOL Multiphysics for conducting detailed simulations. This software is widely recognized for its accuracy in modeling fluid dynamics and heat transfer processes. Also, this software allows to perform coupling between fluid physics and thermodynamics. In this study, conductive and unsteady-

state conduction simulations were performed for the different conditions depending on the stage that was being simulated. For instance, the first and fifth stages comprehended contact only which means also only conductive phenomena. The second and fourth stages involved contact, but also included fluid heat removal the exposure to air. COMSOL allows to use of predefined (or imported) geometries which facilitates the process of specifying the dimensions required for the heart as well as for the different domains in each stage. Moreover, COMSOL Multiphysics allows to carrying out of automatic meshing either user-dependent or physics-dependent meshing. The meshing process can be specified by how small the different parameters are. On the other hand, a mesh independency study was performed to determine the accuracy of the different sizes in contrast with the computational time required for the simulations. Once the meshing conditions were determined, the different stages were set up and the different results plots were created.

2.4 Organ geometry

A detailed three-dimensional model of the heart was created based on anatomical data. The organ geometry included key structures such as chambers and surrounding tissues. This realistic representation ensured the accuracy of the simulations in capturing the complexities of the actual organ. Different geometry parts were ignored to simplify the model.

2.5 Material properties

Physiological material properties, such as thermal conductivity and specific heat, were assigned to different components of the organ model. These properties were obtained

from literature reviews and experimental data to ensure the simulations accurately represented real-world conditions. The value used of thermal conductivity for the heart was $0.5576 W/m \cdot K$, a muscle density of $1080 kg/m^3$ and a value of $3686 J/kg \cdot K$ for the specific heat capacity at constant pressure of the heart. Depending on the stage, there were additional properties included such as the material properties of water and air. The material properties of the bag are assumed to be approximately water properties because the volume occupied by the bag is negligible compared to the volume occupied by the water inside the bag. On the other hand, the external heat transfer resistance from the ambient air to the bag surface was accounted for in simulations in stage 2 and 4, assumed roughly equivalent to the conduction resistance of a thin $2\,mm$ layer of air which gives a conduction resistance of $h \approx 12\,W/m^2\,K$.

2.5.1 Initial Conditions and Boundary Conditions

Simulations were performed under various initial conditions, including different starting temperatures and thermal profiles within the organ. This allowed investigate the impact of the initial state on temperature optimization during the transplant process. The initial conditions for the first stage are determined by understanding how long the heart takes to reach the cardioplegia temperature. Different boundary conditions were applied to simulate scenarios such as variations in ambient temperature, blood flow rates, and cooling mechanisms. Exploring these conditions provided insights into the sensitivity of the temperature optimization process to external factors. Depending on the time that the experimental procedure takes, the temperature at the end of this stage should be different. This case was evaluated using a body temperature of $T_B = 37^oC$ and a cardioplegia temperature of $T_C = 1^oC, T_C = 4^oC, T_C = 10^oC$. The second stage includes initial conditions for the bag and ice temperature. The bag temperature was set to be approximately room temperature of $T_S = 18^oC$. The ice

temperature was assumed to be $T_I = -2^oC$. The heart's initial condition is determined by the equilibrium temperature obtained from the previous stage. Therefore, there were two possible cases evaluated. The two cases evaluated in the second are equilibrium temperature at $t = 10\,min$ and $t = 20\,min$. After the second stage is performed, the ice amount is increased in the system for the third stage following the equilibrium temperature from the second stage and in contact with air at $T_A = 24^oC$. Lastly, the fourth stage and the fifth stage follow the same process but heat the heart. Specifically, these stages use the equilibrium temperatures from the previous stages as well as the material properties of the materials that are included. The fourth stage is comparable to the second and the fifth stage is compared to the first stage.

2.5.2 Iterative simulations

A systematic optimization approach was adopted, involving iterative simulations with adjustments to parameters based on the outcomes of each iteration. This process aimed to converge to the parameters that solve the heat transfer in solids following the quadratic Lagrange discretization process which is a finite differences technique to find solutions to the equations. The simulations were set to include a time-dependent physics model approach which means there was the possibility to specify the time and the range of calculation. For these simulations the time unit used was seconds and the range of output times was between $t = 0s$ and $t = 50000s$. Now, on the other hand, different step sizes were used depending on the simulation and the result of the mesh independency study. Generally, step sizes were located in the rang $[0.01, 10]$ for the simulations. The solutions storage per time was physics-controlled. After each simulation was calculated, different plots were generated to assess the performance and to store useful data for future analysis. In this case, the stored variables were the surface temperature, sliced plots of the geometry, and temperature plots in three

different regions and three different planes. The three regions refer to points located either on the left part of the heart, the right part of the heart, or the middle. The three different planes refer to an upper cut of the geometry, a middle cut, and a lower cut. These allow us to see the temperature distributions depending on the point over the heart.

2.5.3 Performance metrics

The success of each simulation was assessed using performance metrics, including temperature uniformity and adherence to physiological temperature ranges. These metrics allowed for a quantitative evaluation of the effectiveness of different conditions. The first checkpoint for the performance metrics is understanding that the heat or cool-down process takes place following thermodynamic laws and the conditions specified for each stage. Afterward, once the temperature plots are obtained, they are analyzed to address whether the evolution of temperature through time is according to the conditions specified. Finally, the results were compared to temperature values reported by clinicians and from experimental procedures. Once the conditions simulated reflected the experimental conditions reported, there was the possibility of suggesting optimal conditions for that procedure specifically.

2.5.4 Statistical analysis and visualization techniques

Statistical analysis was performed on the simulation results to identify significant trends and correlations. This analysis included regression analyses and sensitivity studies calculating confidence intervals and statistical variables to understand the relationships between various parameters and temperature outcomes. These plots were obtained for the different stages mentioned above as well as for the different geometry partitions.

Also, it was possible to obtain geometry plots showing the temperature distribution and how it evolves in time. This was done using visualization techniques, such as heat maps and temperature profiles. These visual aids facilitated a comprehensive understanding of temperature variations within the heart under different conditions.

Chapter 3

Theoretical Principles

The theoretical principles involved in this proposal are mainly related to transport phenomena processes. This is because the organ (i.e., heart) is in constant contact with different surfaces and materials during the process and there are temperature variations in the system constantly due to different factors. Conduction takes place due to the collisions of molecules. In a continuous medium, Fourier's law states that the conductive heat flow ($\mathbf{q}$) is proportional to the temperature gradient by,

$$\mathbf{q} = -k\nabla T, \tag{3.1}$$

where the proportionality coefficient refers to the thermal conductivity of the material. It takes a positive value meaning the second law of thermodynamics in regards to that the heat flow moves from regions of high temperature to regions of low temperature. Generally, in anisotropic media, the thermal conductivity is defined as a symmetric positive-definite second-order tensor,

$$k = \begin{pmatrix} k_{xx} & k_{xy} & k_{xz} \\ k_{yx} & k_{yy} & k_{yz} \\ k_{zx} & k_{zy} & k_{zz} \end{pmatrix} \tag{3.2}$$

Convection may be due to forced flow (e.g., due to a pump) or flow generated naturally due to temperature differences in a vertical direction (resulting in density differences, hence buoyancy forces). And, radiation is caused by the transport of photons through electromagnetic waves [3] [7]. Now, from the general heat balance equation, it is possible to obtain the heat transfer heat equation in solids interface,

$$\rho C_p \left(\frac{\partial T}{\partial t} + \mathbf{u}_t \cdot \nabla T \right) + \nabla \cdot (\mathbf{q} + \mathbf{q}_r) = -\alpha T : \frac{dS}{dt} + Q. \tag{3.3}$$

In the previous equation, C_p denotes the heat capacity at constant stress, $\mathbf{u}_t$ denotes the velocity vector of translational motion, α denotes the coefficient of thermal expansion, S denotes the second Piola-Kirchhoff stress tensor and Q refers to additional heat sources within the system [7]. It is also assumed that the material properties (ρ, C_p, k) are not temperature dependent for the solid material (heart muscle) specified for the geometry.

When written for the general case of a following fluid, the heat balance equation becomes [3],

$$\rho C_p \left(\frac{\partial T}{\partial t} + \mathbf{u} \cdot \nabla T + \right) + \nabla \cdot (\mathbf{q} + \mathbf{q}_r) = -\frac{1}{\rho} \frac{\partial \rho}{\partial T} \left(\frac{\partial p}{\partial t} + \mathbf{u} \cdot \nabla p \right) + \tau : \nabla \mathbf{u} + Q. \tag{3.4}$$

The previous equation may be solved numerically to obtain quantitative results in COMSOL, considering also that most of its terms may be consider negligible for the needs of this work. This includes the three velocity terms (due to absence of fluid

flow), the radiation term (since no significant radiation heat transfer is expected) and the additional heat source term (since no heat generation of any type takes place within the boundaries of the system). Therefore, the above equation is simplified to,

$$\rho C_p \frac{\partial T}{\partial t} + \nabla \cdot \mathbf{q} = 0. \tag{3.5}$$

Assuming that the heart tissue is thermally isotropic (i.e., the thermal conductivity is the same in all directions),

$$\rho C_p \frac{\partial T}{\partial t} + \nabla \cdot (-k \nabla T) = 0. \tag{3.6}$$

Which gives,

$$\rho C_p \frac{\partial T}{\partial t} - k \nabla^2 T = 0. \tag{3.7}$$

This is the simplified equation used to solve the heat transfer taking place in the heart transplantation processes in this study. As said before, this model has simplifications and can be perfected including additional heat sources and dependencies that exist during the process such as blood flowing through the geometry, additional materials in geometry domains and temperature dependence of material properties. Depending on the stage that is being solved, there are different initial values and boundary conditions. For the first stage, the initial values and boundary conditions are,

$$T_{\partial\Omega}(t = 0) = 37^o C. \tag{3.8}$$

$$T_{\Omega(-)} = 1^o C. \tag{3.9}$$

The initial values and boundary conditions for the second stage depends on which timeline is being solved. T_S denotes the bag temperature and the surface notion refers

to the heart itself. If in this stage the heart is not considered to be submerged in ice then,

$$T_S(t=0) = 18^oC. \tag{3.10}$$

$$T_{\partial\Omega}(t=0) = T_{C_{eq}}(t = 10min, 20min). \tag{3.11}$$

However, if ice is included in the geometry such as it is in the second timeline,

$$T_S(t=0) = 18^oC. \tag{3.12}$$

$$T_I(t=0) = -2^oC. \tag{3.13}$$

$$T_{\partial\Omega}(t=0) = T_{C_{eq}}(t = 10min, 20min). \tag{3.14}$$

And, on the other hand,

$$q = h_A(T_A - T_{\partial\Omega}). \tag{3.15}$$

For the third stage, the initial values for the simulations are,

$$T_S(t=0) = T_{eq}(t = 10min, 20min). \tag{3.16}$$

$$T_H(t=0) = T_{eq}(t = 10min, 20min). \tag{3.17}$$

$$T_I(t=0) = -2^oC. \tag{3.18}$$

$$T_A(t=0) = 24^oC. \tag{3.19}$$

Similarly, as the second stage, the fourth stage conditions depend on the timeline simulated. If in this stage the heart is not considered to be submerged in ice then,

$$T_S(t=0) = 18^oC. \tag{3.20}$$

$$T_{\partial\Omega}(t=0) = T_{eq}(t = 10min, 20min). \tag{3.21}$$

However, if ice is included in the geometry such as it is in the second timeline,

$$T_S(t=0) = 18^oC. \tag{3.22}$$

$$T_I(t=0) = -2^oC. \tag{3.23}$$

$$T_{\partial\Omega}(t=0) = T_{eq}(t = 10min, 20min). \tag{3.24}$$

And, on the other hand,

$$q = h_A(T_A - T_{\partial\Omega}). \tag{3.25}$$

Lastly, for the fifth stage, the initial values and boundary conditions are,

$$T_\Omega(t=0) = T_{eq}(t = 10min, 20min). \tag{3.26}$$

$$T_{\Omega(-)} = 37^oC. \tag{3.27}$$

The following figure summarizes the notation for the boundary conditions for each domain.

Finally, the following tables show the materials and properties assumed for each stage.

Stage 1 - Cardioplegia Process			
Location / Material	$k(W/m \cdot K)$	$C_p(J/kgK)$	$\rho(kg/m^3)$
Heart Muscle	0.56	3686	1080

Table 3.1: Properties values for the cardioplegia simulations.

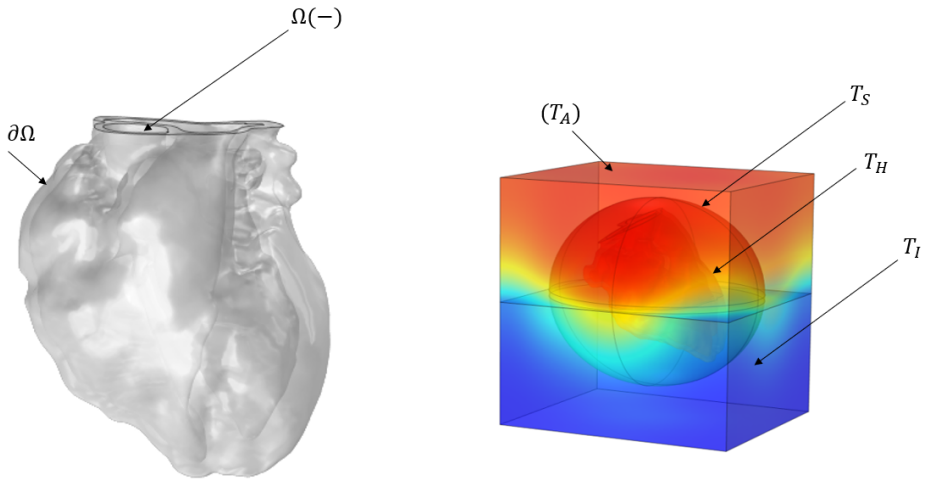

Figure 3.1: Notation specified for each domain in the boundary conditions and initial values equations.

Stage 2 - Back Table			
Location / Material	$k(W/m \cdot K)$	$C_p(J/kg \cdot K)$	$\rho(kg/m^3)$
Heart Muscle	0.56	3686	1080
Water	0.598	4181	997

Table 3.2: Properties values for the back-table simulations.

Stage 3 - Ice box storage			
Location / Material	$k(W/m \cdot K)$	$C_p(J/kg \cdot K)$	$\rho(kg/m^3)$
Heart Muscle	0.56	3686	1080
Water	0.598	4181	997
Air	0.03	1000	1.29

Table 3.3: Properties values for the ice box storage simulations.

Stage 4 - Back Table			
Location / Material	$k(W/m \cdot K)$	$C_p(J/kg \cdot K)$	$\rho(kg/m^3)$
Heart Muscle	0.56	3686	1080
Water	0.598	4181	997

Table 3.4: Properties values for the back-table simulations.

Stage 5 -Warm-up Process			
Location / Material	$k(W/m \cdot K)$	$C_p(J/kgK)$	$\rho(kg/m^3)$
Heart Muscle	0.56	3686	1080

Table 3.5: Properties values for the warm-up simulations.

Chapter 4

Computational Modeling

This chapter describes the process by which the simulations were executed starting with the software that is being used. Afterward, it is explained the modules that were used in predicting the behavior of the physical properties in the model. Also, there is an explanation to address the reasons why the heart geometry was refined and also to justify carrying out a mesh independence study. Finally, each of the stage sections shows the results obtained for each part of the process including the temperature plots and the distributions obtained both in temperature, isothermal contours, and sliced geometry plots. Furthermore, additional features of each simulation are given so that the data can be replicated and to allow further studies in this matter.

COMSOL Multiphysics was chosen to be the software in which the simulations were carried out. This is not only due to its ability to deal with CFD simulations but also because it includes multiple modules that are useful in this particular project. For instance, modules that were useful during the geometry refinement process and also because they use detailed model meshing parameters and adjust to complex geometries. Now, on the other hand, COMSOL can include different physics modules that

could be coupled inside one single simulation. In this case, the simulation was specified to be carried out following the equations in the heat transfer module defining domains, boundary conditions, and initial conditions for the different stages of the heart transplantation process.

Also, COMSOL allows for varying parameters during the meshing process and records the computational time and step size for each simulation. This is important for executing a mesh independence study and determining the most accurate mesh for the geometry without losing accuracy in the results obtained in the simulations. Also, the time required to run the simulations varied depending on the solutions that were saved in different step sizes. This was taken into account so that the frames that were saved reflected the physical phenomena that were taking place.

4.1 Geometry

The geometry used for the models is a heart-shaped STL file geometry which represents an initial approach in the solids heat transfer models. The purpose of cutting the geometry in the way it is shown in figure 4.1 is because the initial objective is to see how the heat transfer takes place within the heart and includes different domains. Also, the cut allows to define the boundary conditions and the initial values for each of the domains.

The heart geometry was processed in COMSOL Multiphysics specifying the dimensions which would match with a heart dimension. The heart volume for the modeled geometry is $2.85 \cdot 10^{-4}\ m^3 \approx 285 cm^3$. For stage 2 and stage 4, the bag size is assumed to be $2 \times 10^{-3}\ m^3$ and the ice volume is set to be $2.4 \times 10^{-3}\ m^3$. For stage 3, the ice

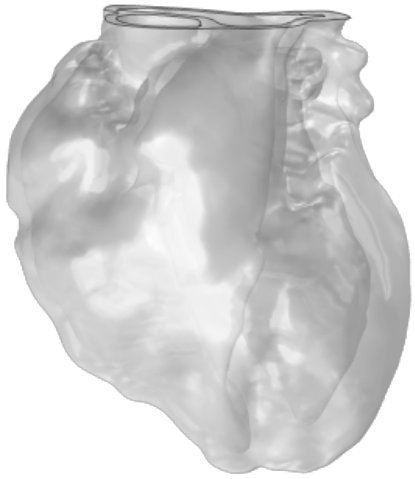

Figure 4.1: Heart-shaped geometry used to perform heat transfer in solid configurations.

volume is increased from $2.4 \times 10^{-3}\ m^3$ to $3.13 \times 10^{-3}\ m^3$.

4.2 Mesh

Meshing is an important feature in the execution of these simulations. Especially, because using complex geometries could lead to easier divergences and could affect the accuracy of the results. COMSOL Multiphysics performs an automatic meshing specifying the size of each of the elements in the mesh. The purpose of meshing is to solve the differential equations that govern the specified physics over the domains. In this case, the physics refers to heat transfer equations in solids. However, the smaller element size does not mean that the results would be more accurate. That is why it is important to carry out a mesh independence study in which the computational time is

compared to the mesh element size to obtain comparable results. Figure 5.7 shows the mesh obtained with a fine element size as an example of how the geometry is meshed and shows the fine element size performed over the geometry used for the simulations.

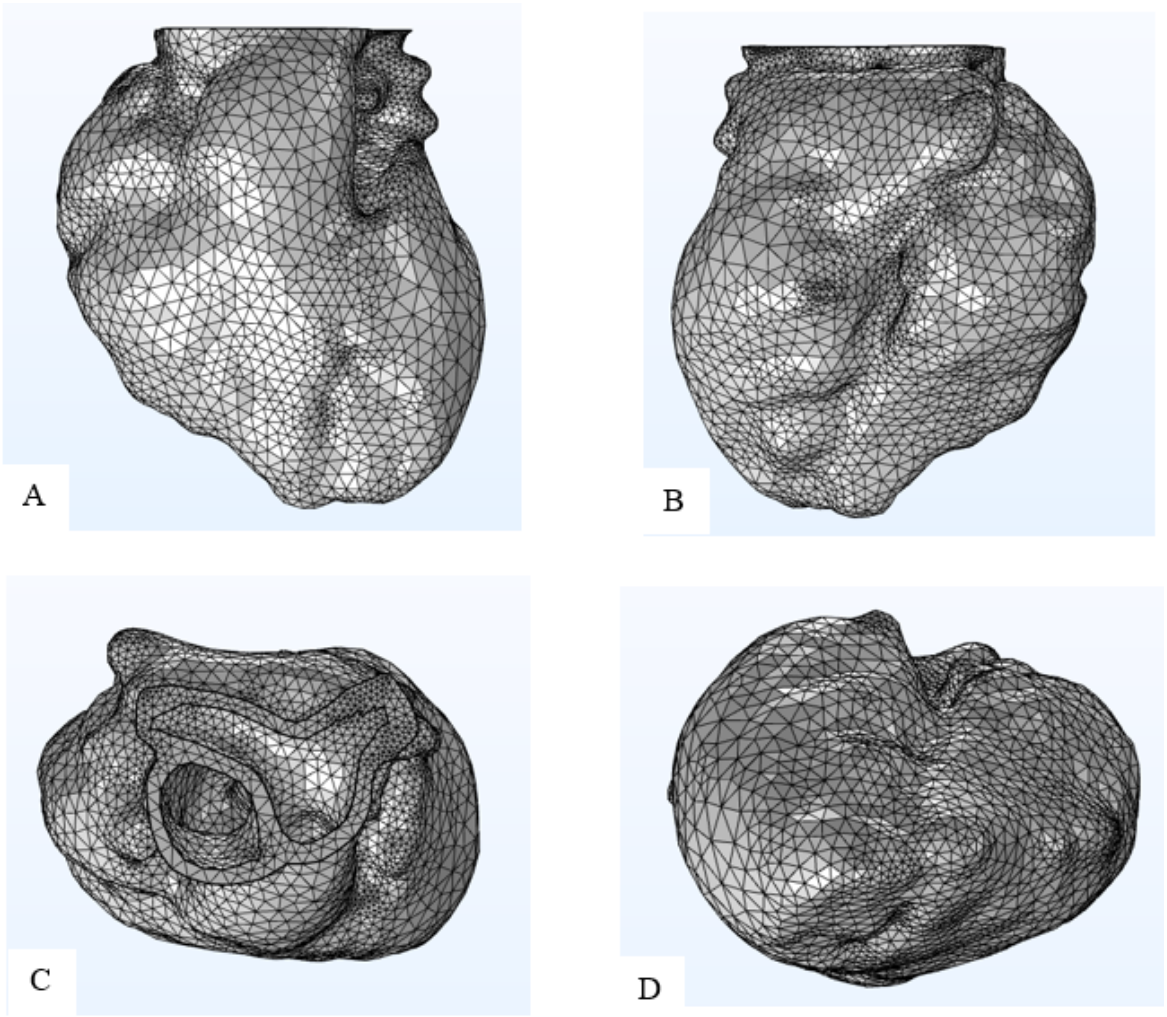

Figure 4.2: Heart meshing result using a Fine element size and a physics-controlled mesh in COMSOL Multiphysics. (A) frame shows a frontal view. (B) frame shows a back view. (C) shows an upper view and (D) shows a bottom view. These views are evidence that there are no divergences in the mesh execution.

4.3 Mesh Independence Study

A mesh independence study is performed to balance the computational time required for a simulation and the accuracy of the results obtained. Particularly, the type of mesh was changed according to the specified mesh categories specified in COMSOL. It was set that the meshing process was physics-controlled mesh so that COMSOL performs an automated approach to generate the mesh. In COMSOL, the mesh quality indicates the length and width ratio of the elements for a specific geometry. If the mesh quality is ideal, the value of this value is 1. But, argumentatively, if the geometry has anisotropic dimensions, the mesh quality decreases. The number of elements generated for the first stage oscillated between 5000 and 200000 elements. Each of the mesh studies shows the quality element histogram which determines the quality of the mesh based on the area under the curve. That area is set to be the element quality in (%). Since the mesh independence balances the results obtained, it is shown that the element quality does not change significantly after 3.5 seconds for the first stage. Then, a fine category mesh is an accurate approach independent of the number of elements generated. Figure 4.3 shows the results obtained for the first stage. On the other hand, different temperature plots for obtained for three different meshes for the first stage. Figure 4.4 shows those results for coarse, fine, and finer mesh. The coarse results show a strong deviation compared to the finer meshes which does not make it an accurate mesh for the simulations even though it does take less time to run. However, the extremely fine meshes show a small temperature data deviation from the average finer mesh, but it takes a considerably long time to run. Therefore, a finer mesh would be an accurate approach to balance the computational time and the accuracy of the results obtained.

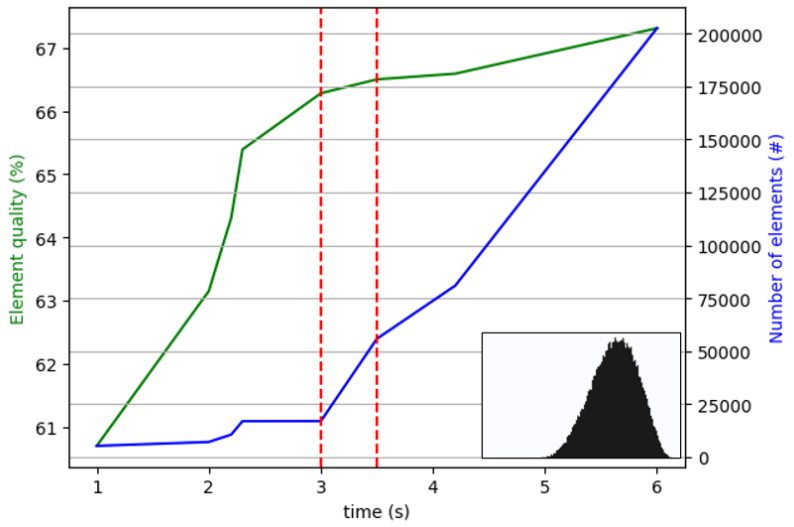

Figure 4.3: Mesh independency graph for the mesh performed in the first stage. The graph shows the element quality calculated for the different mesh categories, the number of elements obtained, and the time to mesh the anisotropic heart geometry.

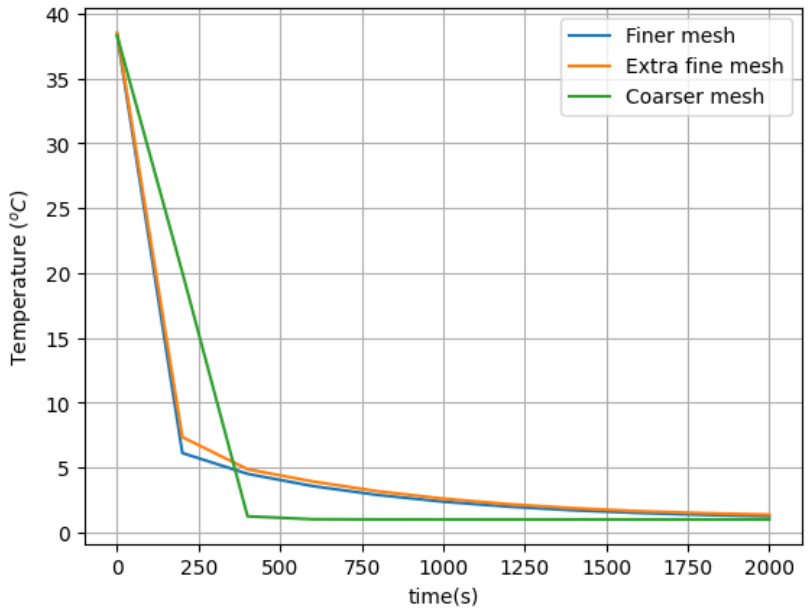

Figure 4.4: Temperature results obtained for an evaluation case of the mesh independency. It is possible to see that finer meshes do not necessarily show more accurate results. Also, coarser meshes do not take longer than finer meshes but the results lose accuracy comparably.

Chapter 5

Results

5.1 Stage 1 - Cardioplegia process

The simulated cardioplegia takes place when the heart is cooled down using a fluid pumped throughout the system. In this case, since the simulation is performed with the solid heat transfer conditions, it is directly assumed that the fluid in the system is stationary and carries out the temperature specified in all its domains. This means that the simulations evaluate how long the heart takes to reach the specified temperature. This stage was run for three different cardioplegia temperatures: $T_C = 1^oC$, $T_C = 4^oC$, and $T_C = 10^oC$. For each of the temperatures, the time evolution for each cardioplegia temperature is shown in figures 5.1, 5.2, and 5.3. It is possible to obtain sliced plots of the geometry as well. Figure 5.4 shows the temperature distribution and sliced plots for T_C of 1^oC as an example. Finally, figure 5.6, 5.7 and 5.8 show the temperature plots obtained for the different regions of the heart and different temperatures.

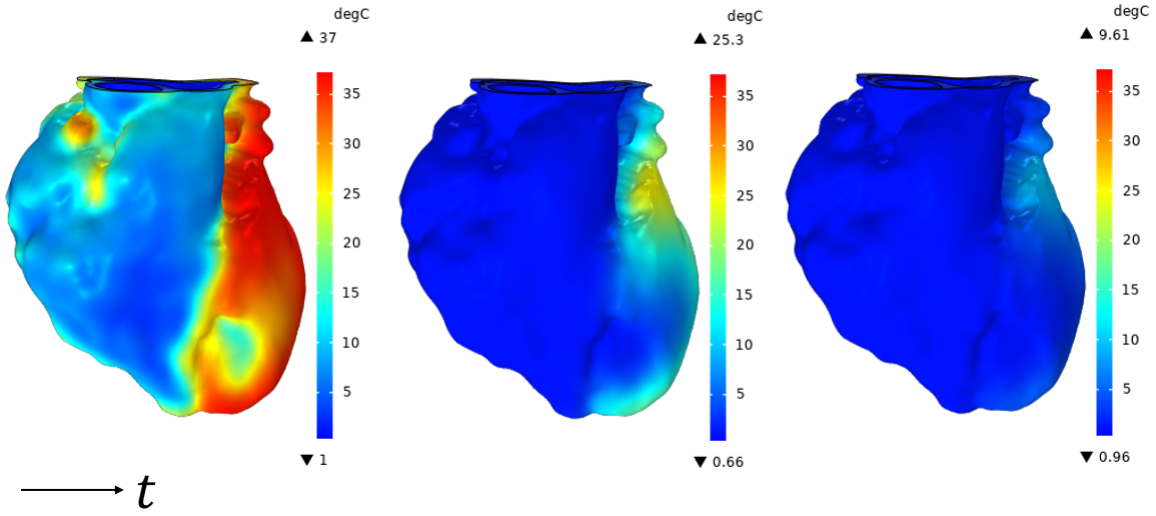

Figure 5.1: Cardioplegia simulations for $T_C = 1^oC$. The left frame shows the temperature distribution at $t = 1\,min$. The middle frame shows the distribution at $t = 10\,min$. The right frame shows the temperature distribution at $t = 20\,min$.

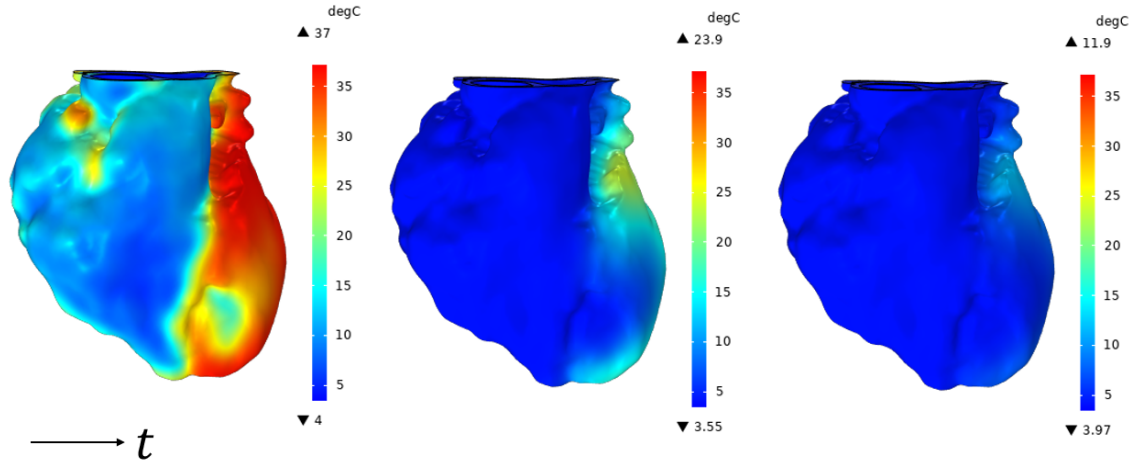

Figure 5.2: Cardioplegia simulations for $T_C = 4^oC$. The left frame shows the temperature distribution at $t = 1\,min$. The middle frame shows the distribution at $t = 10\,min$. The right frame shows the temperature distribution at $t = 20\,min$.

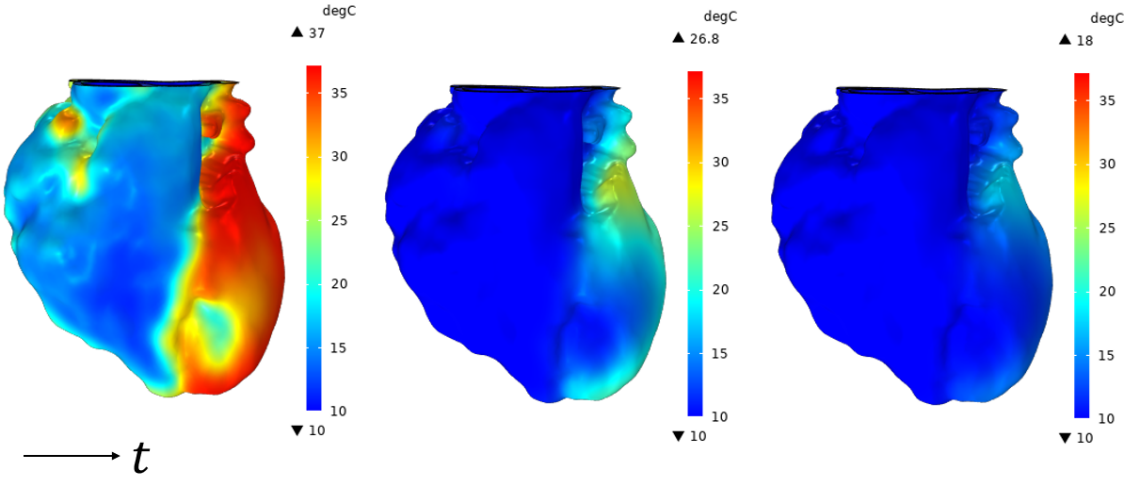

Figure 5.3: Cardioplegia simulations for $T_C = 10^oC$. The left frame shows the temperature distribution at $t = 1min$. The middle frame shows the distribution at $t = 10min$. The right frame shows the temperature distribution at $t = 20\,min$.

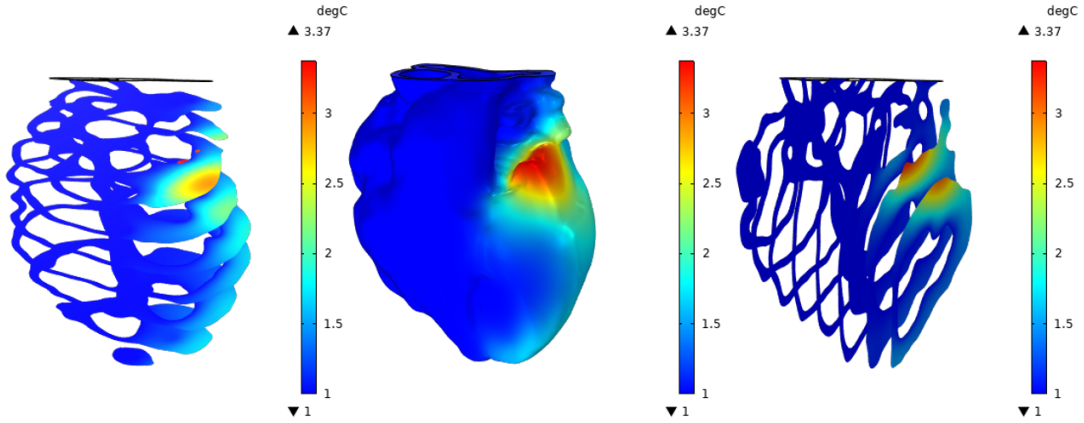

Figure 5.4: Temperature distribution and sliced plots for a cardioplegia process performed with a water solution at $T_C = 1^oC$. It is possible to see the horizontally sliced plot, the temperature distribution, and the vertically sliced plot from left to right. These plots were obtained for a specific time $t = 5\,min$ as an example.

Now, on the other hand, the following figure shows sliced plots as an example of were the different points were located. Specifically, it shows the location of three points for a middle cut of the geometry to plot the temperature evolution of the heart.

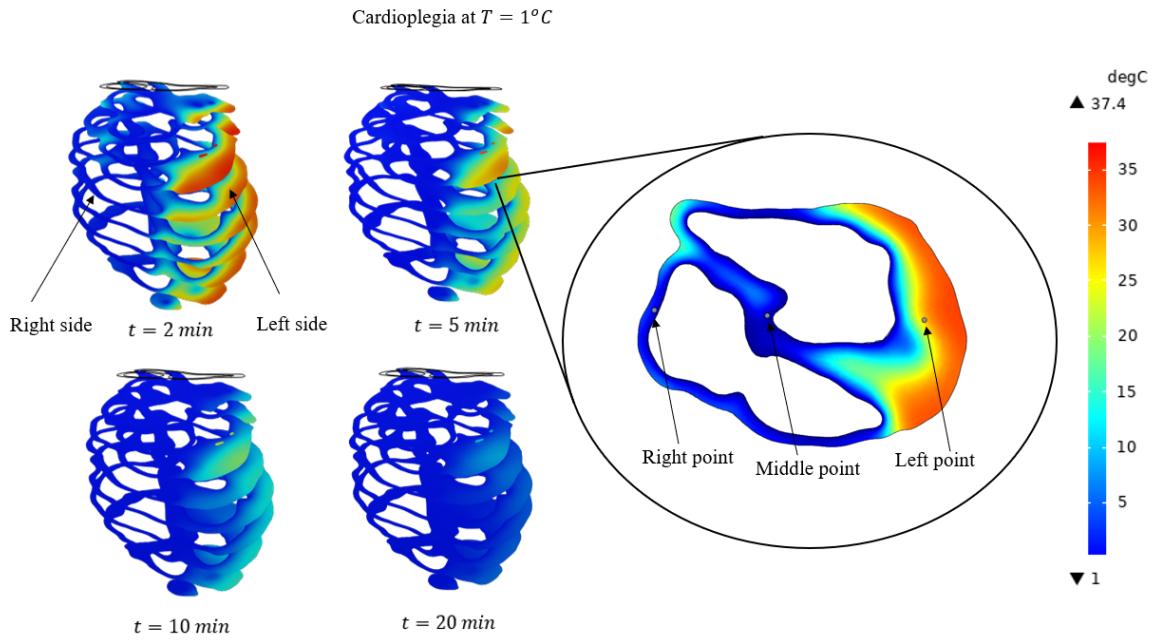

Figure 5.5: Sliced plots were obtained for the cardioplegia simulations at $T_C = 1^oC$ at different times. It shows the location of three points for a middle cut of the geometry to plot left-side temperature evolution, middle-temperature evolution, and right-side temperature evolution.

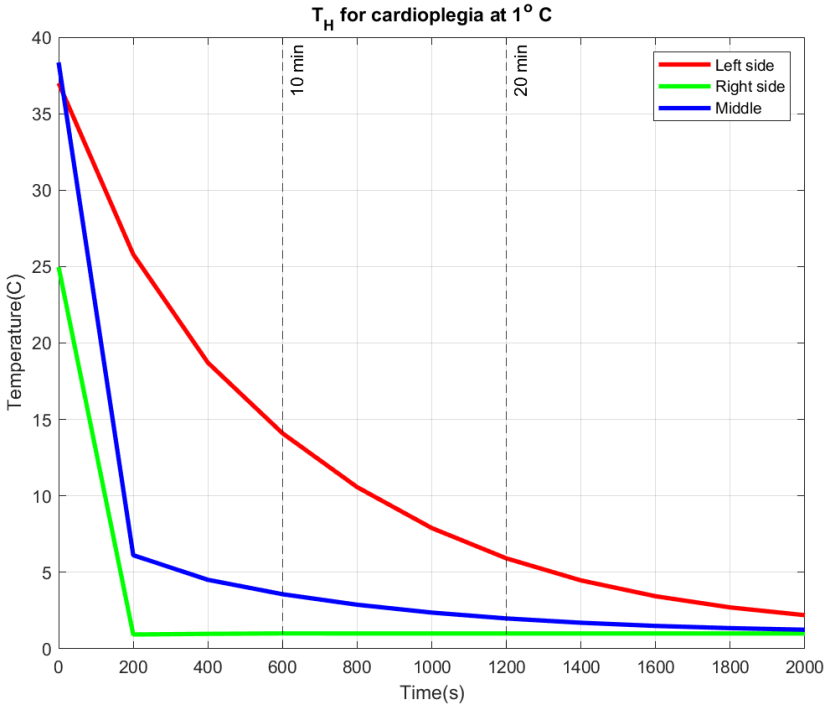

Figure 5.6: Temperature plot for $T_C = 1^oC$.

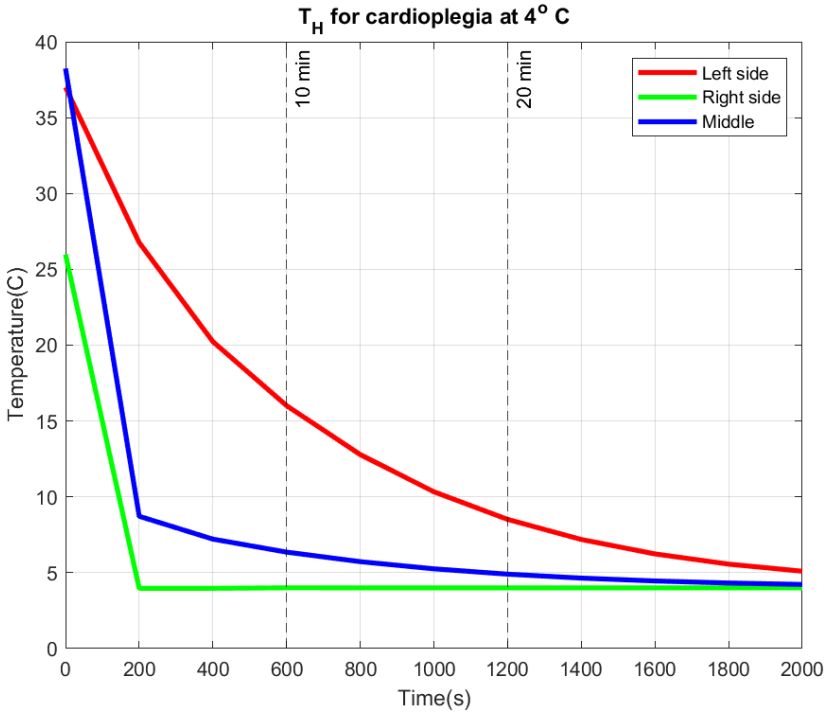

Figure 5.7: Temperature plot for $T_C = 4^oC$.

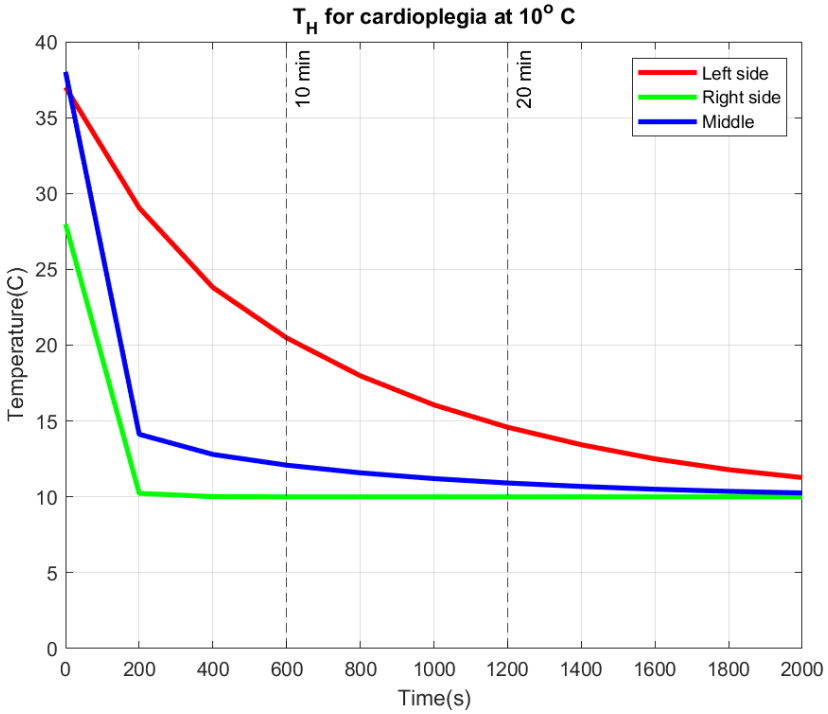

Figure 5.8: Temperature plot for $T_C = 10^oC$.

It is possible to see that if the cardioplegia temperature decreases, the equilibrium temperature reached by the heart at the end of the process is lower. The duration of the experimental process allows the heart to reach either a warmer or a cooler temperature, but it is possible to affirm that this equilibrium temperature will be lower if the temperature of the cardioplegia decreases. Also, it is important to mention that since the heart has thicker and thinner parts in its distribution, some regions take faster to cool down than other regions. As it is seen, the left side of the heart is thicker and therefore, takes more time to cool down. However, the right side of the heart cools down faster than the left side of the heart. Based on the results of the cardioplegia stage, the averaged temperature of the heart for $t = 10\,min$ and $t = 20\,min$ is used as an initial condition for the next stage. The following stages as subdivided into two cases. The first case evaluates just conduction phenomena between the different materials involved. The second case evaluates conduction and it includes

a external heat transfer resistance due to the configuration. Those cases are labeled as the conduction simulations section and the conduction and heat resistance simulations section.

5.2 Conduction simulations approach

5.2.1 Stage 2: Organ back-table stage

The second stage is simulated assuming that the heart is being stored in a bag with a solution of water which is also assumed to be in mechanical equilibrium so that it can be simulated as a solid during the process. Following the simulations pathway, there will be six different results for this stage because each cardioplegia temperature can be completed in either $t = 10\,min$ or $t = 20\,min$. The initial value for the heart temperature is the equilibrium stage reached in the previous stage and the initial temperature of the bag system is assumed to be room temperature at $T_A = 24^oC$. Figure 5.9 shows the results obtained for $t = 10\,min$ with a cardioplegia performed at $T_C = 1^oC$ and Figure 5.10 shows the plots obtained for each temperature. It is possible to affirm that this heat-up process is changing the temperature of the heart from temperatures below 10^oC on average to temperatures close to room temperature. However, the ice box storage will be a key factor in determining if the heart reaches critical temperatures based on the conditions in which it is stored. Also, it is important to mention that this geometry showed a more even heat-up evolution compared to a cool-down evolution regarding the different heart regions simulated.

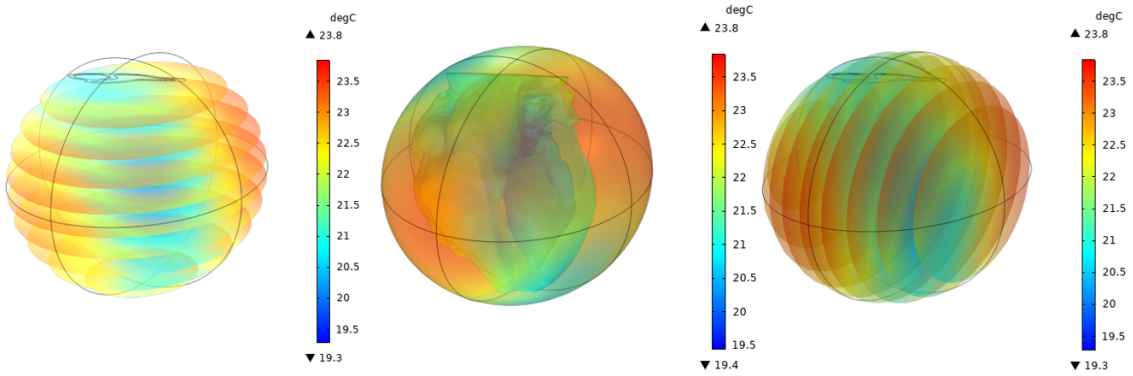

Figure 5.9: Temperature distribution for the back-table process performed after $T_C = 1^oC$ during $t = 10min$. It is possible to see the horizontally sliced plot, the temperature distribution, and the vertically sliced plot from left to right.

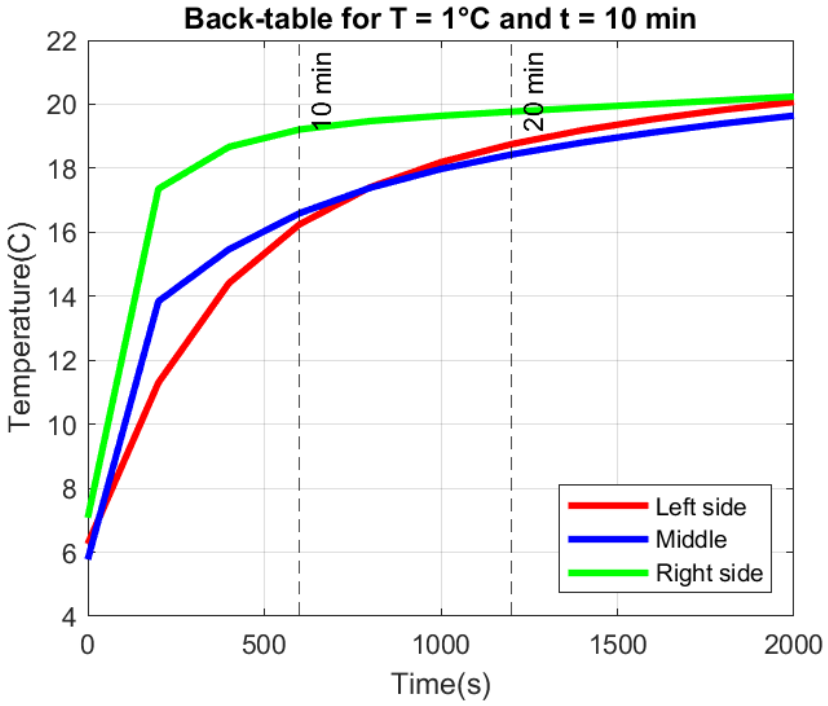

Figure 5.10: Back-table (S_2) temperature plots after a $T_C = 1^oC$ and a time of $t = 10min$.

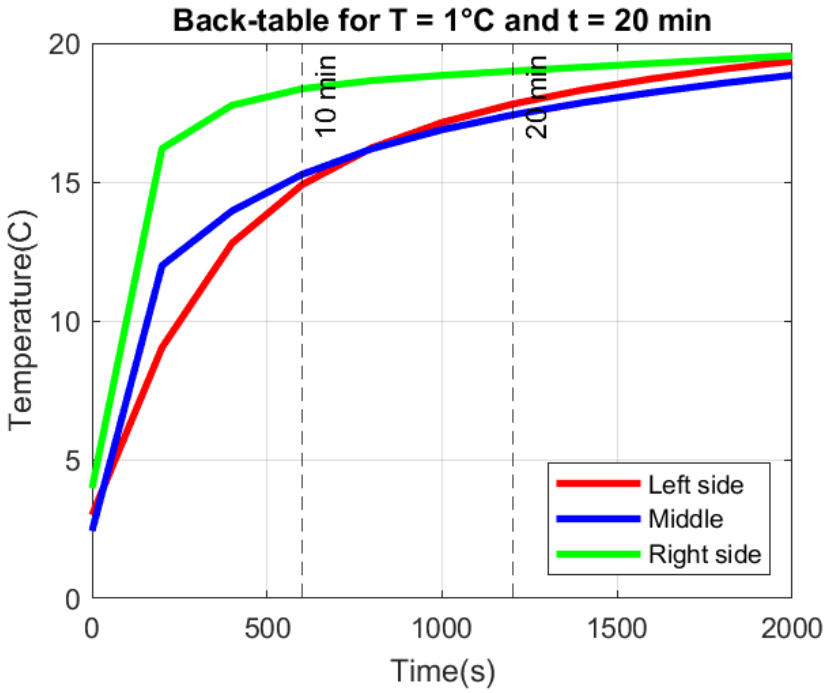

Figure 5.11: Back-table (S_2) temperature plots after a $T_C = 1^oC$ and a time of $t = 20min$.

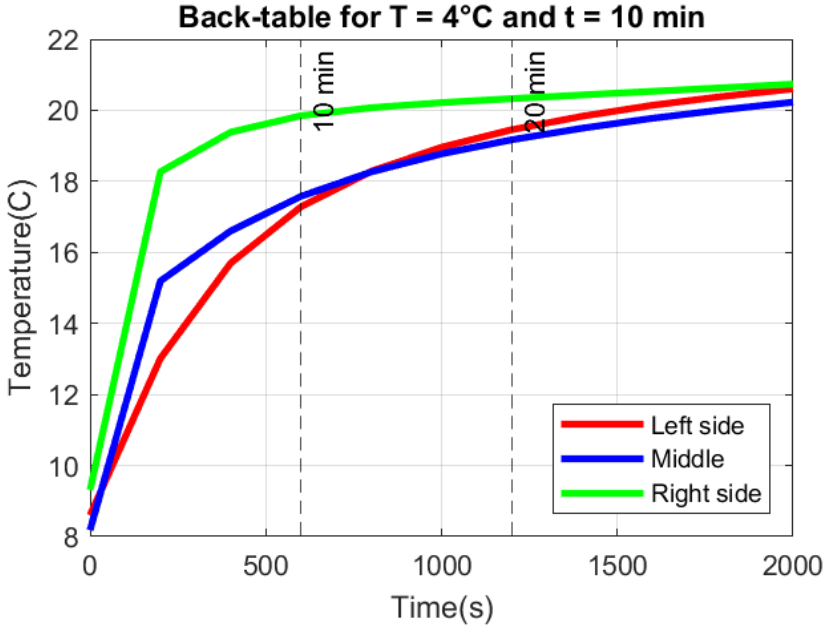

Figure 5.12: Back-table (S_2) temperature plots after a $T_C = 4^oC$ and a time of $t = 10min$.

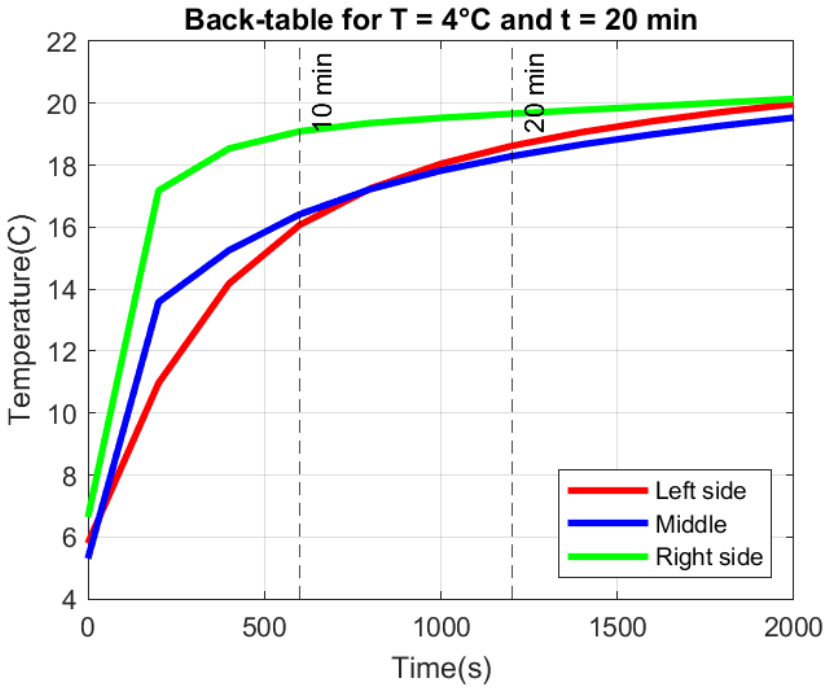

Figure 5.13: Back-table (S_2) temperature plots after a $T_C = 4^oC$ and a time of $t = 20min$.

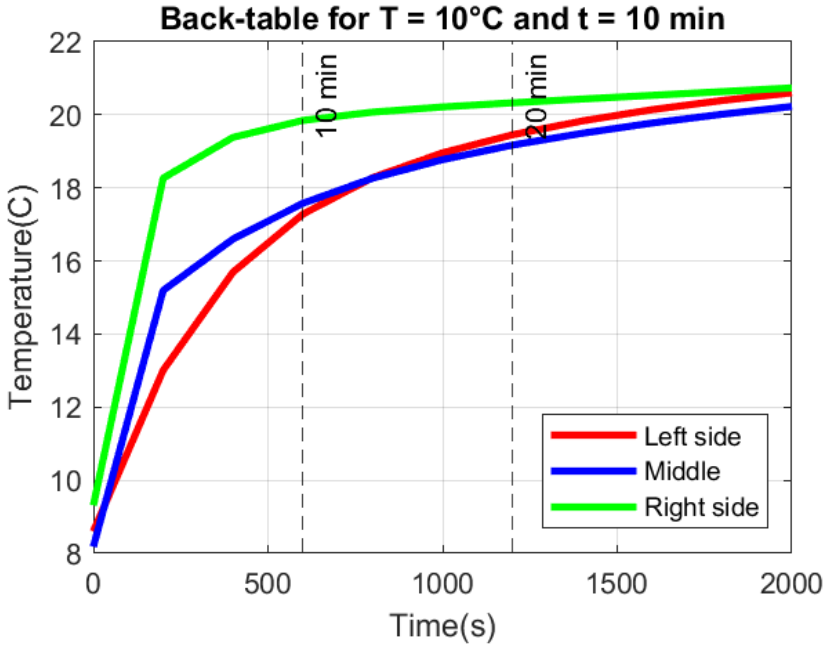

Figure 5.14: Back-table (S_2) temperature plots after a $T_C = 10^oC$ and a time of $t = 10min$.

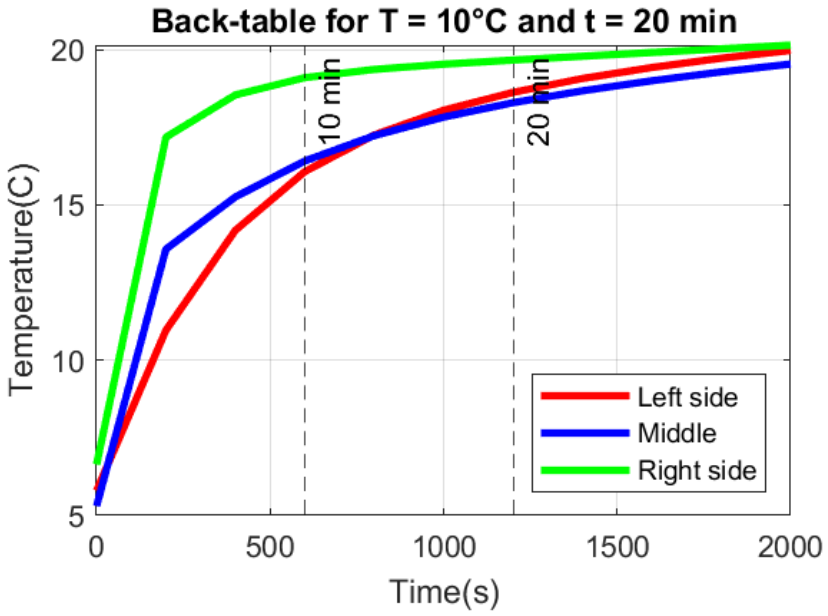

Figure 5.15: Back-table (S_2) temperature plots after a $T_C = 10^oC$ and a time of $t = 20min$.

5.2.2 Stage 3: Ice box storage

After the back-table storage takes place, the organ goes through an ice box storage that takes different times depending on the experimental process. In this case, it was simulated to take up to $t = 4h$. It was assumed that the ice box storage proportion concerning the air insulation was 50%. This means that half of the geometry is filled with ice and half of it is considered to be air as an insulation layer. Figure 5.16 shows the temperature distribution for the ice box storage and Figure 5.17 shows how is the temperature evolution in the middle plane of the heart at different times. After $30\,min$, the heart has been already exposed to an extreme temperature gradient as is seen in the second figure specifically.

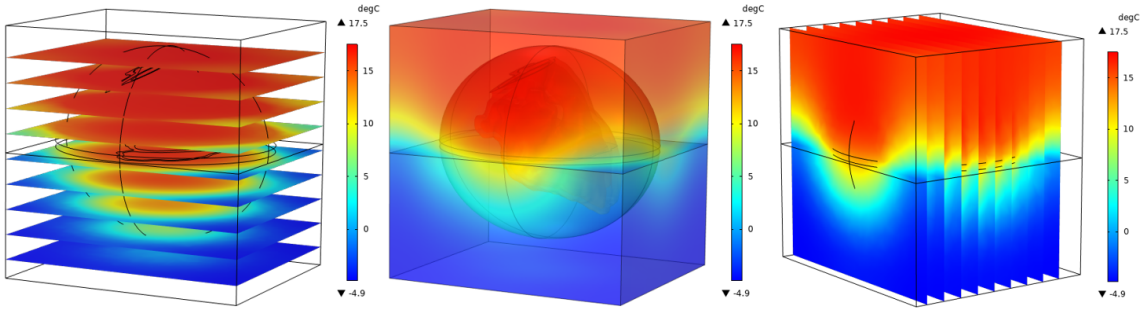

Figure 5.16: Temperature distribution for the ice box storage process performed after a $T_C = 1^oC$ during $t = 10\,min$. It is possible to see the horizontally sliced plot, the temperature distribution, and the vertically sliced plot from left to right.

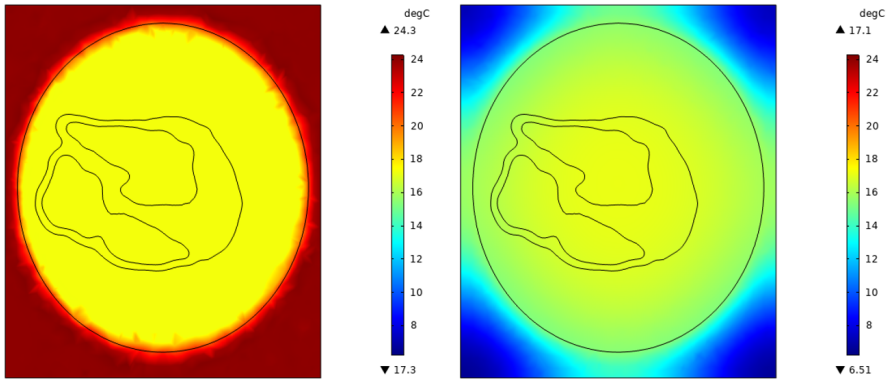

Figure 5.17: Temperature evolution for the ice box storage process at a middle plane for the heart after a $T_C = 1^oC$ during $t = 10min$. The left plane shows the temperature distribution at $t = 0s$ and the right plane shows the temperature distribution at $t = 30\,min$.

Figure 5.18 shows the temperature plots for each case simulated. It is possible to see that there is an even cool-down process throughout all the regions in the heart. Additionally, if the heart starts from the final temperature at the back-table bag storage, which is approximately 18^oC, it takes longer to cool down compared to the time that was simulated. This means that different conditions might be required to achieve critical temperatures in the organ storage.

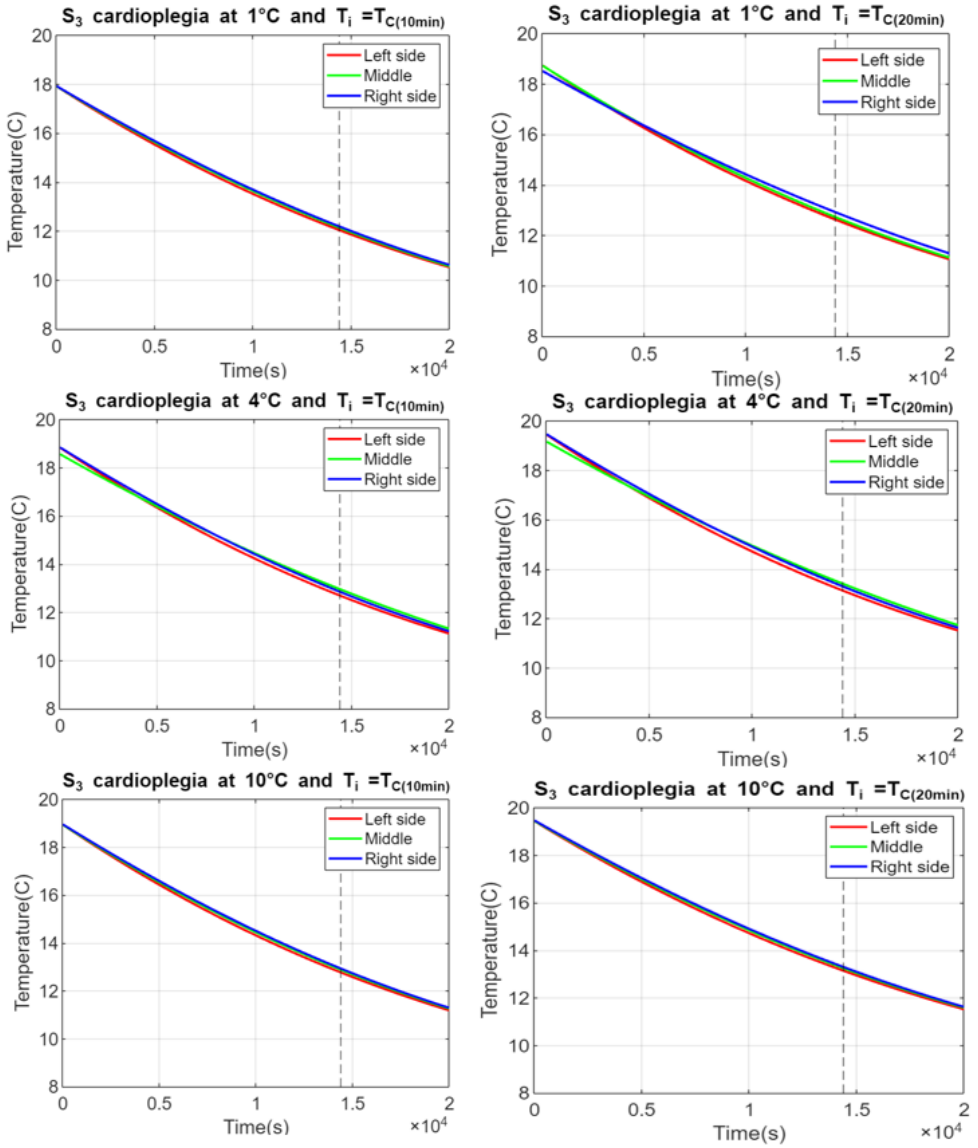

Figure 5.18: Ice box storage (S_3) temperature plots for the three different T_C temperatures and different times of execution during the first stage. The dotted line refers to a heart that has been stored for $t = 4h$.

5.2.3 Stage 4: Back-table stage

After the ice box storage takes place, the heart is removed from the ice, and the bag is placed on a surface. The same assumptions performed at the second stage were assumed here and the final temperatures for the third stage at $t = 10\,min$ and $t = 20\,min$ are the initial temperature values for these simulations. Compared to the previous stage, these simulations are different because there is a heat-up process for the organ that is being stored. And, therefore, the final temperature reached at different times can be also different. Figure 5.19 shows the temperature distribution obtained for this process and particularly shows the heat-up process that takes place if the heart is in contact with air at room temperature. Moreover, the following figures show the different temperature plots obtained for this stage for each case simulated.

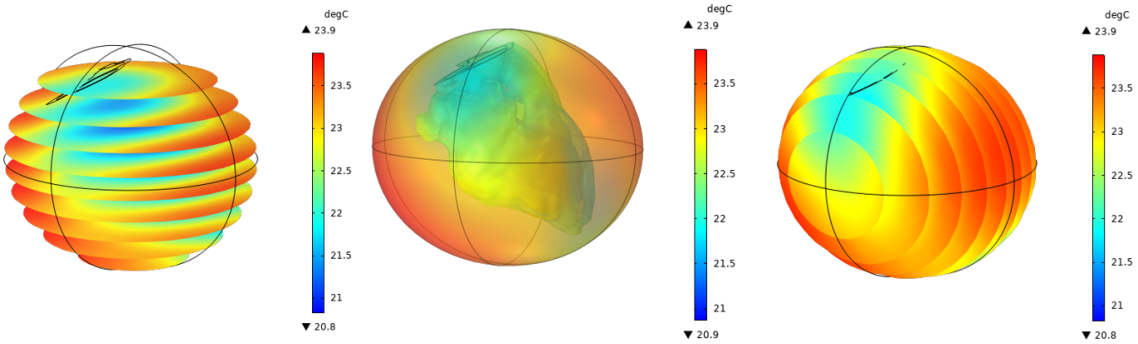

Figure 5.19: Temperature distribution for the back-table bag storage process performed after ice box storage. It is possible to see the horizontally sliced plot, the temperature distribution, and the vertically sliced plot from left to right.

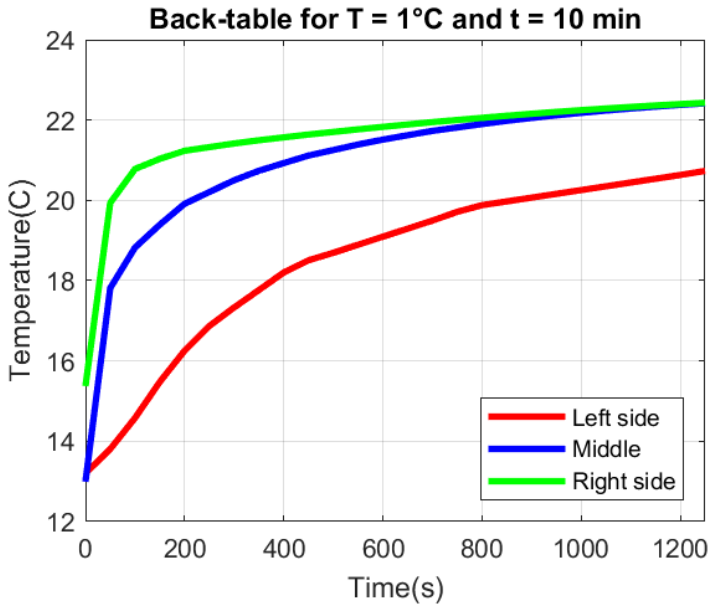

Figure 5.20: Back-table (S_4) temperature plots for a $T_C = 1^oC$ and a second stage execution time of $10\,min$.

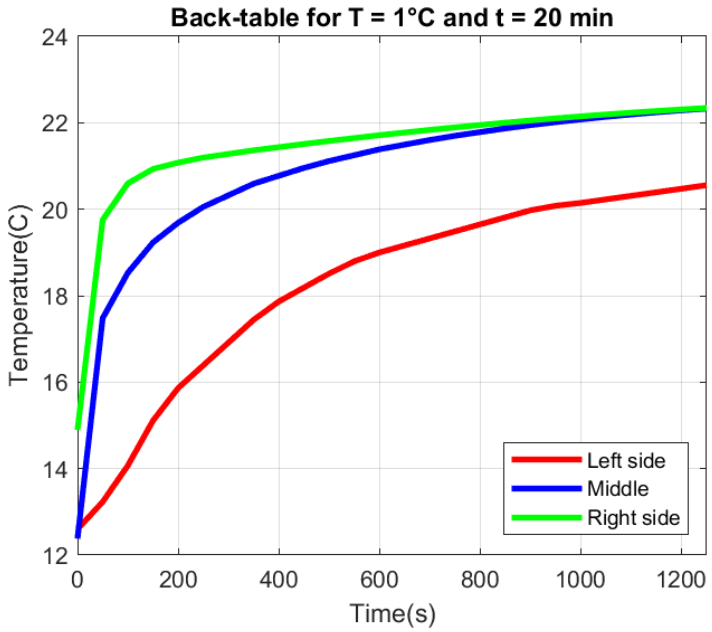

Figure 5.21: Back-table (S_4) temperature plots for a $T_C = 1^oC$ and a second stage execution time of $20\,min$.

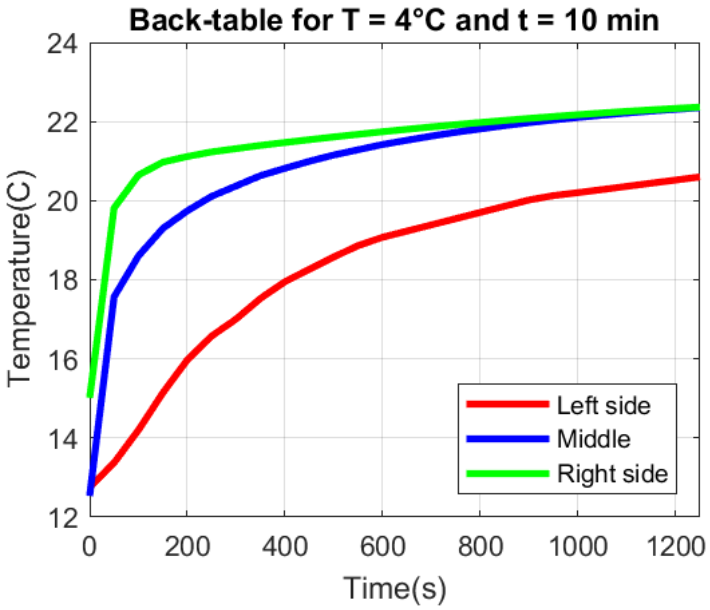

Figure 5.22: Back-table (S_4) temperature plots for a $T_C = 4^oC$ and a second stage execution time of 10 min.

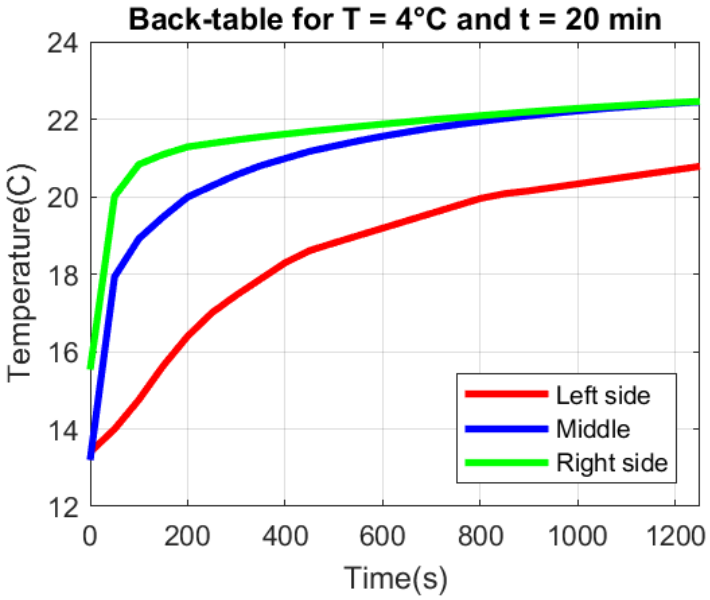

Figure 5.23: Back-table (S_4) temperature plots for a $T_C = 4^oC$ and a second stage execution time of 20 min.

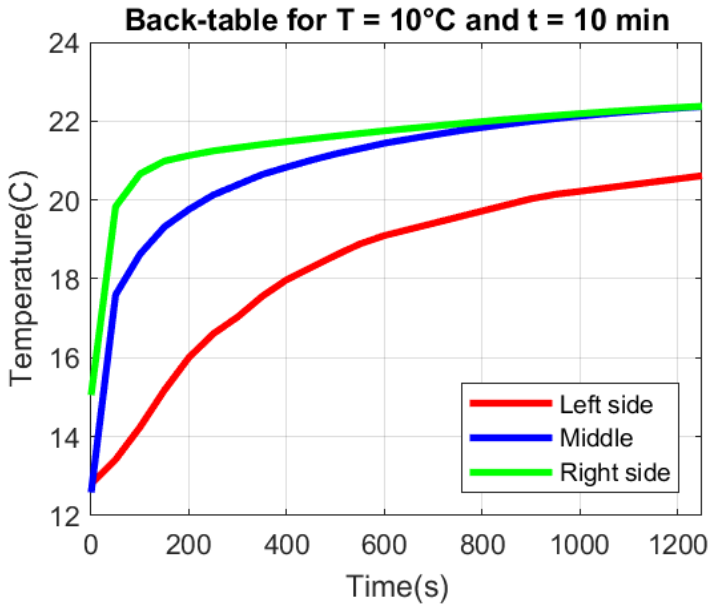

Figure 5.24: Back-table (S_4) temperature plots for a $T_C = 10^oC$ and a second stage execution time of 10 min.

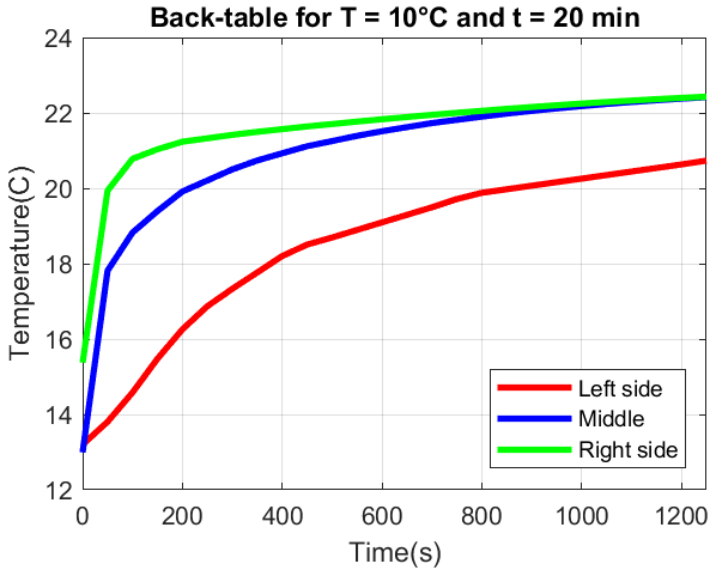

Figure 5.25: Back-table (S_4) temperature plots for a $T_C = 10^oC$ and a second stage execution time of 20 min.

5.2.4 Stage 5: Organ warm-up process

Stage 5 refers to the final stage of the process in which the heart is heated up back to a body temperature of 37^oC. Figure 5.26 shows the temperature distributions obtained for this process as well as the sliced plots showing how this process took place. Similarly, the following figures show the temperature plots for this simulation and they show that heating the heart takes longer than the 20 $mins$ shown to reach body temperatures.

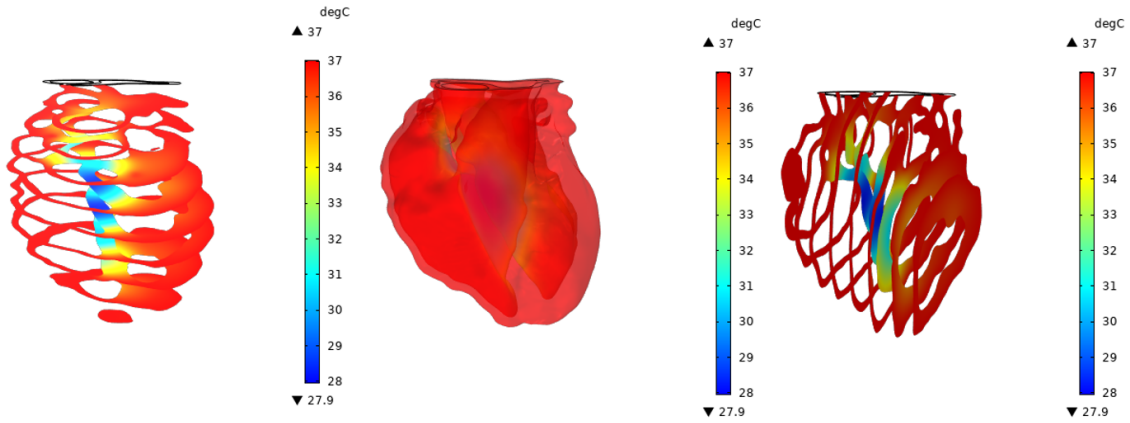

Figure 5.26: Temperature distribution for the heat-up process carried out in the final stage of the heart transplantation process. It is possible to see the horizontally sliced plot, the temperature distribution, and the vertically sliced plot from left to right.

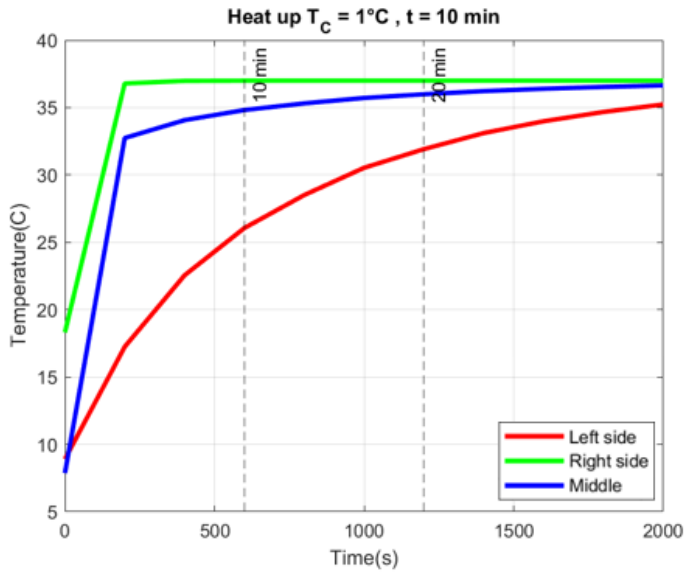

Figure 5.27: Warm-up temperature plots obtained for $T_C = 1^oC$ and a second stage execution time of $10\,min$.

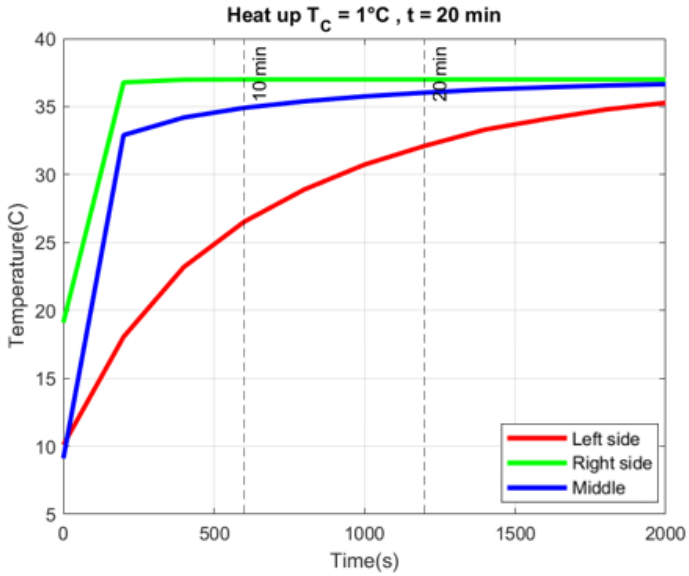

Figure 5.28: Warm-up temperature plots obtained for $T_C = 1^oC$ and a second stage execution time of $20\,min$.

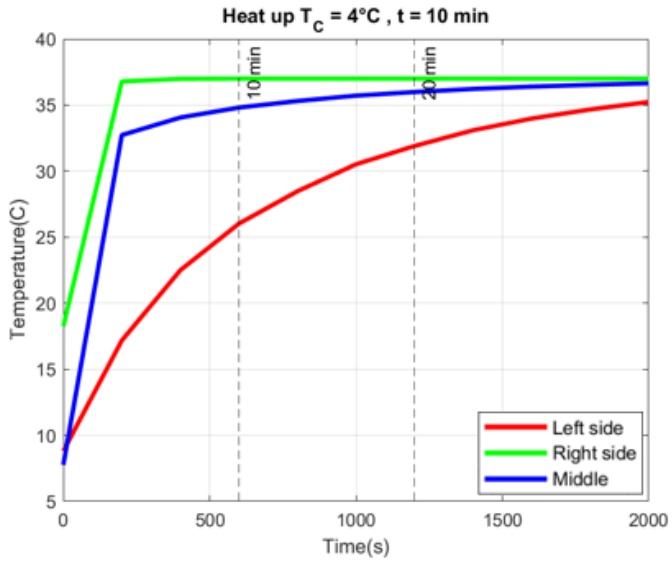

Figure 5.29: Warm-up temperature plots obtained for $T_C = 4^oC$ and a second stage execution time of 10 min.

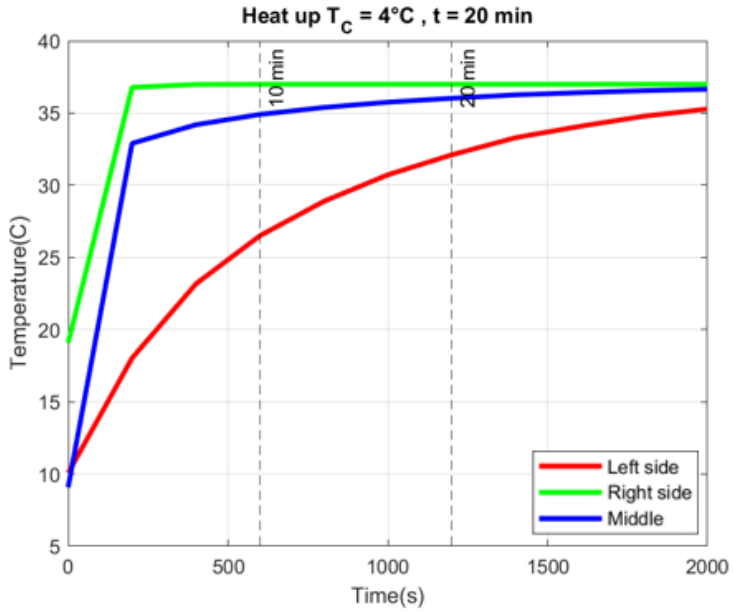

Figure 5.30: Warm-up temperature plots obtained for $T_C = 4^oC$ and a second stage execution time of 20 min.

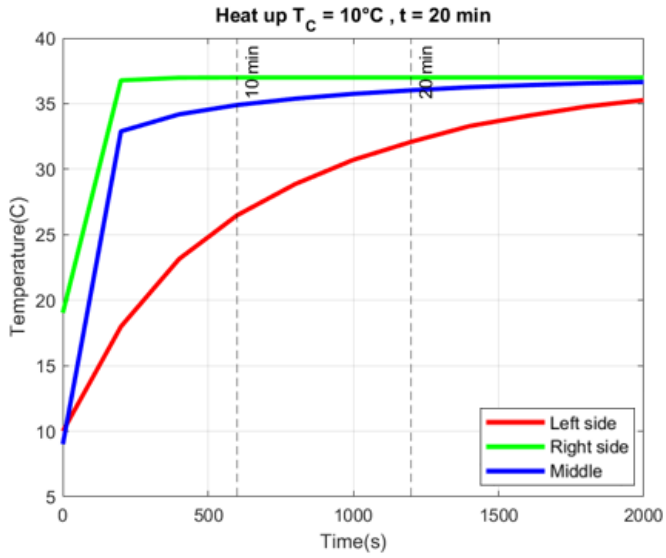

Figure 5.31: Warm-up temperature plots obtained for $T_C = 10^oC$ and a second stage execution time of 10 min.

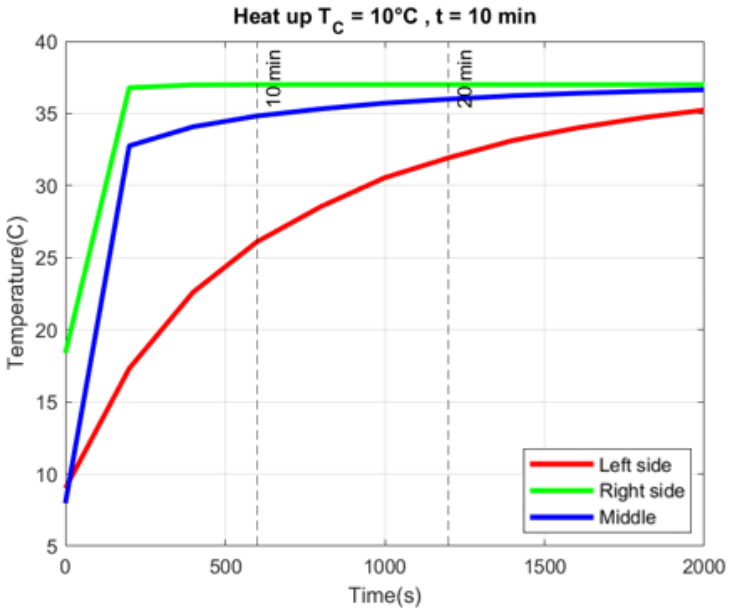

Figure 5.32: Warm-up temperature plots obtained for $T_C = 10^oC$ and a second stage execution time of 20 min.

5.3 Conduction and external heat transfer resistance simulations approach

5.3.1 Stage 2: Organ back-table bag storage

As mentioned above, the second stage of the process refers to the storage of the heart in a bag which includes a fluid solution in it. This bag is paced over ice which means there are conduction and an external heat transfer resistance. The solution inside the bag was assumed to be liquid water as was done in the previous second-stage simulation. In this simulation case, the second stage includes ice half-filled in comparison to the previous simulations. Also, the bag dimensions were adjusted close to the heart shape enough so that it resembles contact with the surface of a normal bag. Conduction phenomena refers to the contact that exists between the heart and the bag and the bag and the ice. This means that there is a creation of new domains in comparison to the first stage. The ice geometry was assumed to be a regular cube neglecting the effects of pointy geometries and empty regions in ice placement distributions. Figure 5.33 shows the geometry setup for the second stage as well as the time evolution for the case of cardioplegia executed at $T_C = 1^oC$ and time of execution of $t = 10\,min$.

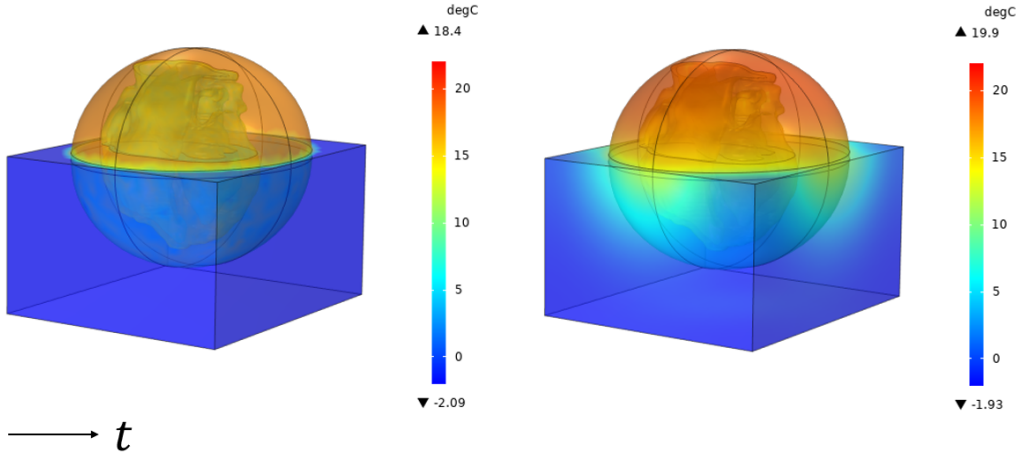

Figure 5.33: Back-table bag storage time evolution plot for the temperature distribution for $T_C = 1^oC$ and $t = 10\,min$. The temperature distribution obtained evaluates conduction heat transfer among heart equilibrium temperatures for the first stage, the bag temperature, and the ice temperature. The heat transfer through heat resistance phenomena is assumed to follow Newton's law. The first frame is for $t = 0\,min$ and the second frame is for $t = 10\,min$.

The following figures show that during the back-table bag storage process, the heart follows a not significant heat-up process due to the thermodynamic competition between the initial bag temperature and the ice temperature which half fills the geometry as shown in Figure 5.33. In other words, since the bag temperature is approximately room temperature, it competes with cooler temperatures such as ice temperatures and combined they do not affect significantly the heart. In this case, assuming a cardioplegia temperature of $T_C = 1^oC$ and that it took $t = 10min$, it is possible to see that, on average, the heart reached an equilibrium temperature not greater than $+10^oC$ if the process of putting the heart in the bag takes less than $t = 20min$. Also, the equilibrium temperature obtained at the end of this second stage would be the initial condition for the next stage and it is a temperature greater than those temperatures reported to affect heart tissue performance.

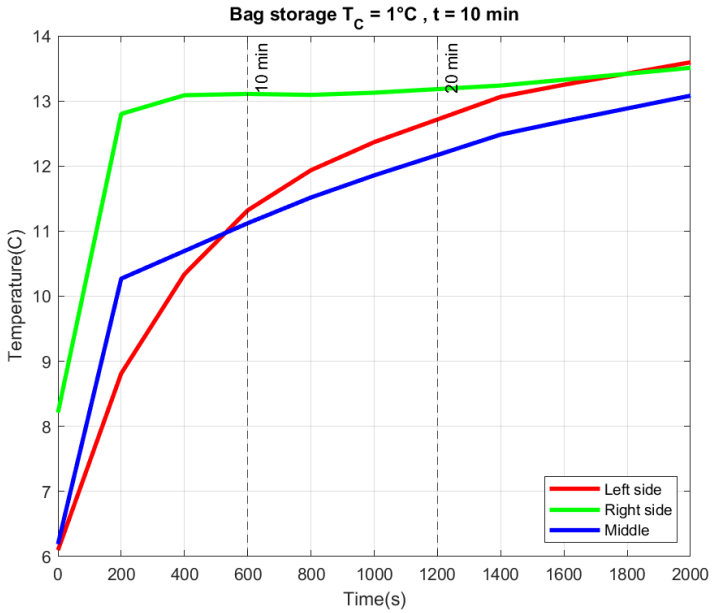

Figure 5.34: Back-table for $T_C = 1^oC$ and duration of $t = 10\,min$.

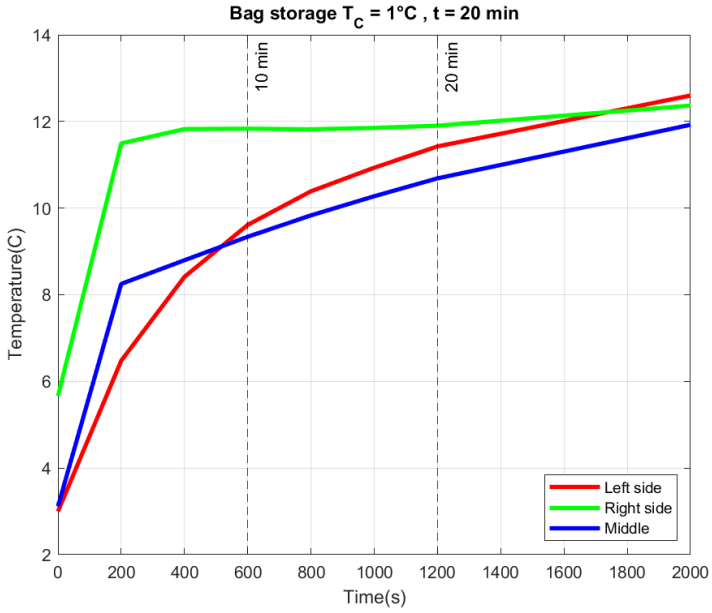

Figure 5.35: Back-table for $T_C = 1^oC$ and duration of $t = 20\,min$.

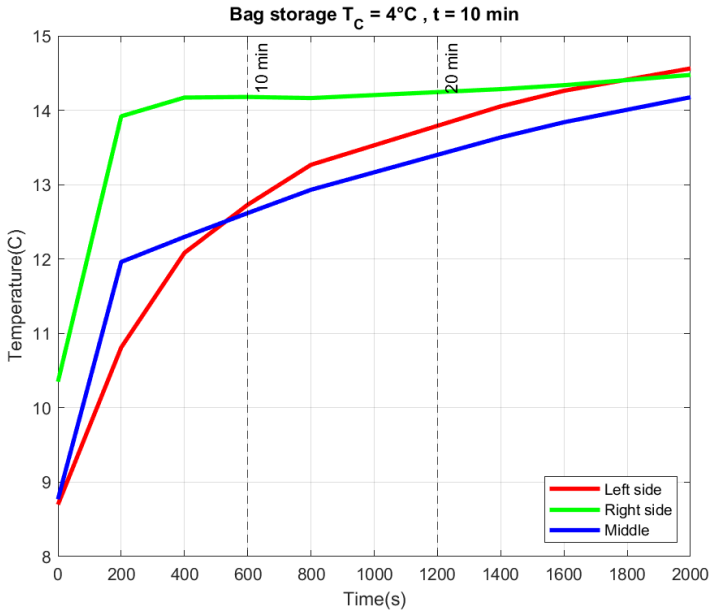

Figure 5.36: Back-table for $T_C = 4^oC$ and duration of $t = 10\,min$.

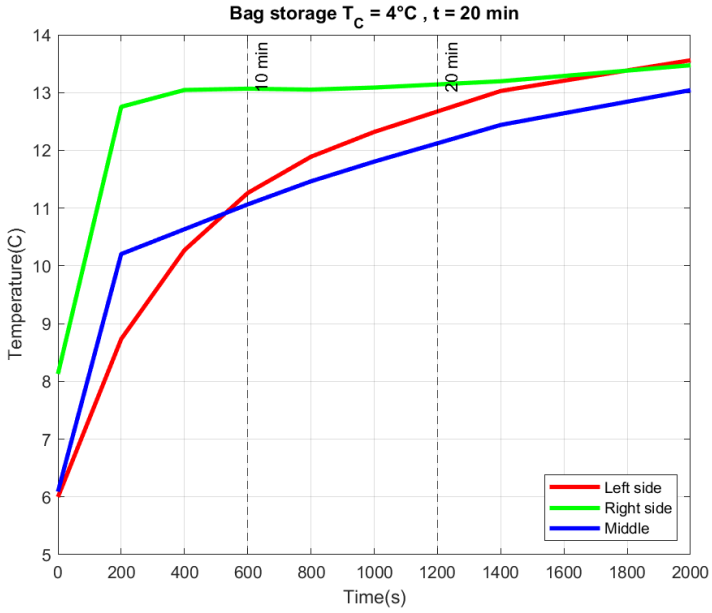

Figure 5.37: Back-table for $T_C = 4^oC$ and duration of $t = 20\,min$.

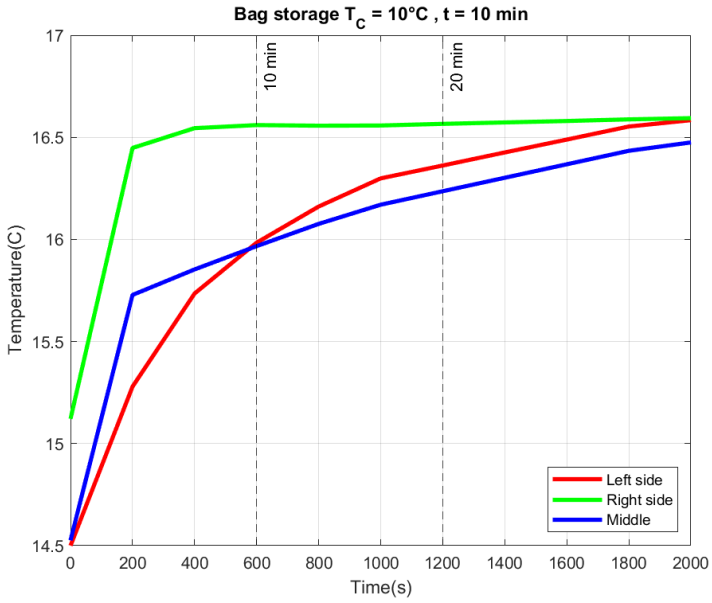

Figure 5.38: Back-table for $T_C = 10^oC$ and duration of $t = 10\,min$.

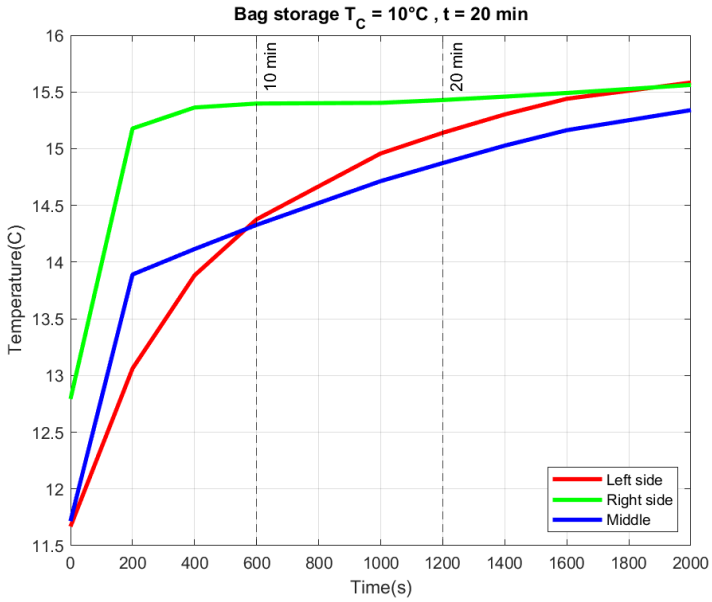

Figure 5.39: Back-table for $T_C = 10^oC$ and duration of $t = 20\,min$.

5.3.2 Stage 3: Ice box storage

The third stage of the process is the storage of the heart in an icebox which is filled with ice until the point in which most of the heart is submerged. In this case, since the

ice box is a closed environment, the external heat transfer resistance phenomena is not considered. Instead, there is an insulator air layer on top of the ice domain covering the rest of the geometry. However, conduction phenomena are taking place in this stage between the different domains. The dimensions were adjusted to resemble the dimensions used experimentally during heart transplants. It is expected that there will be a considerable temperature drop in this stage due to the ice temperature. Again, the ice geometry was assumed to be a regular cube neglecting pointy geometry effects and empty regions in ice placement distributions. Figure 5.40 shows the geometry setup for the third stage. It is important to mention that the simulation was run for a total time of $t = 6h$ which is higher than the time for the previous simulations. This means that this stage assumes that the heart was stored under those conditions at that time. The ice temperature assumed for this stage was $T_I = -2^oC$. The air layer temperature was assumed to be room temperature at $T_A = 24^oC$. The case shown is the distribution temperature simulated for a cardioplegia performed in the first stage at $T_C = 1^oC$ and time of execution of $t = 10\,min$. The additional surface plot combinations for the other cardioplegia temperatures are included.

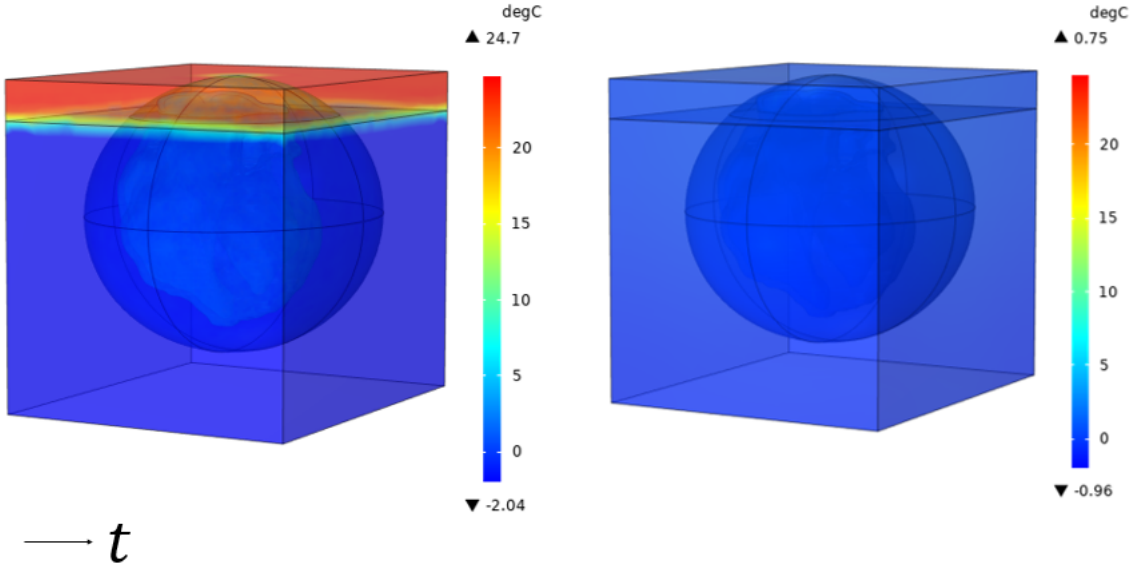

Figure 5.40: Ice box storage simulation for $T_C = 1^oC$ and $t = 10min$. The temperature distribution obtained evaluates conduction heat transfer for the equilibrium temperatures of the previous stage, the bag, and the ice temperatures. The first frame is for $t = 0\,min$ and the second frame is after $t = 6\,h$.

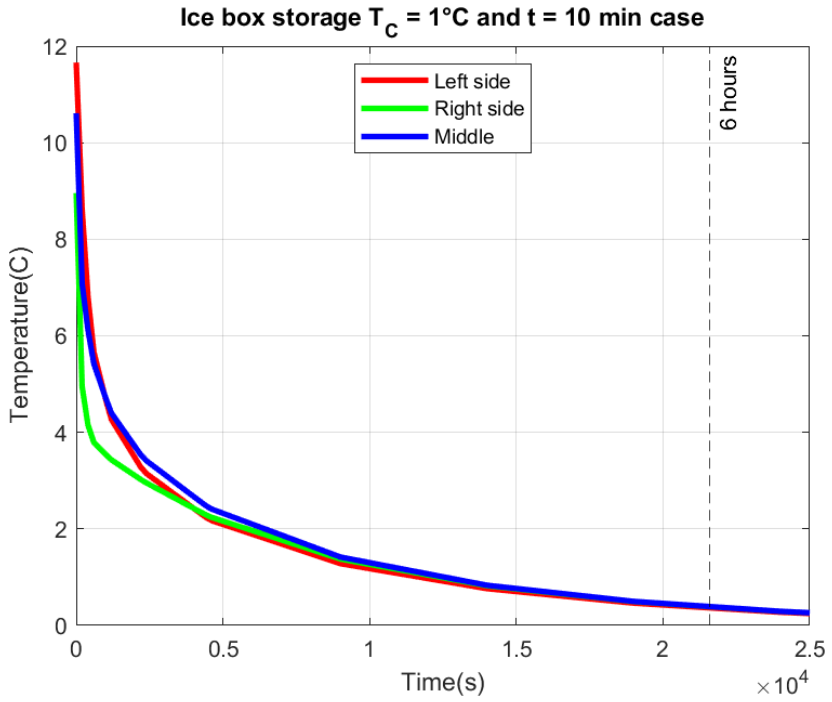

Figure 5.41: Ice box temperature plot for $T_C = 1^oC$ and second stage duration of $10\,min$.

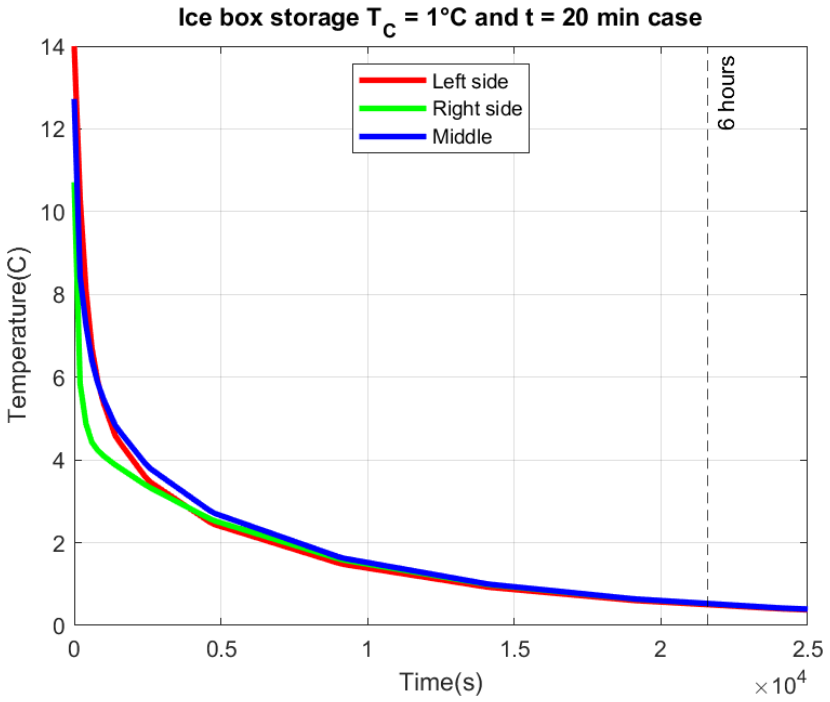

Figure 5.42: Ice box temperature plot for $T_C = 1^oC$ and second stage duration of 20 min.

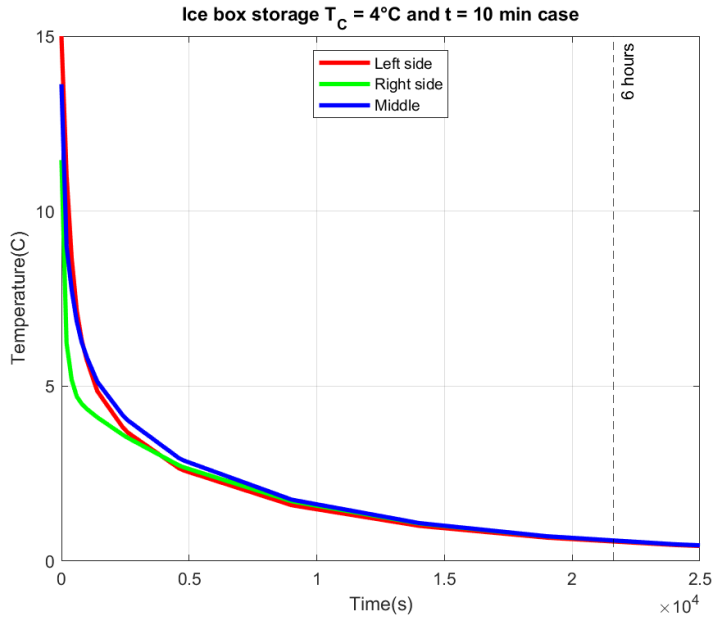

Figure 5.43: Ice box temperature plot for $T_C = 4^oC$ and second stage duration of 10 min.

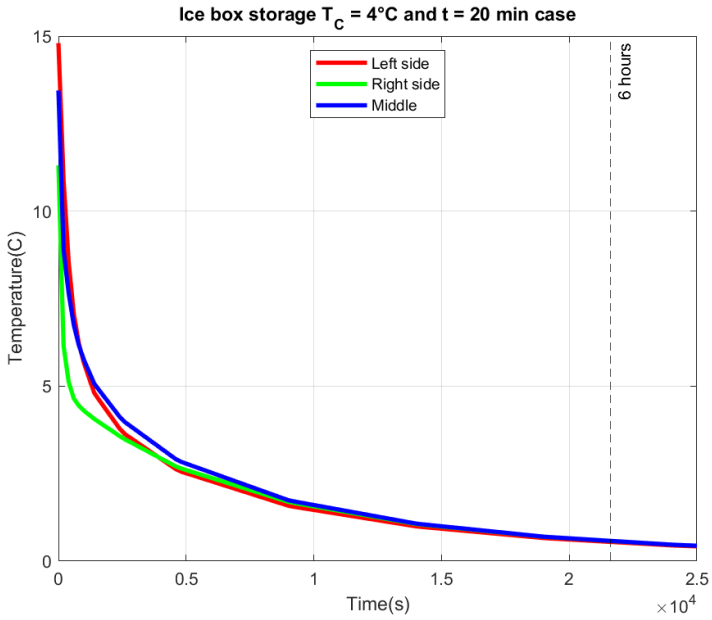

Figure 5.44: Ice box temperature plot for $T_C = 4^oC$ and second stage duration of 20 min.

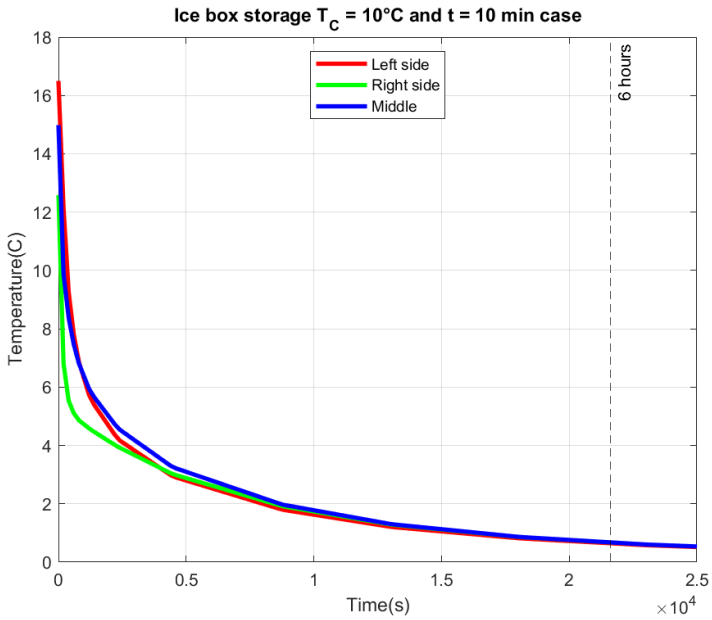

Figure 5.45: Ice box temperature plot for $T_C = 10^oC$ and second stage duration of 10 min.

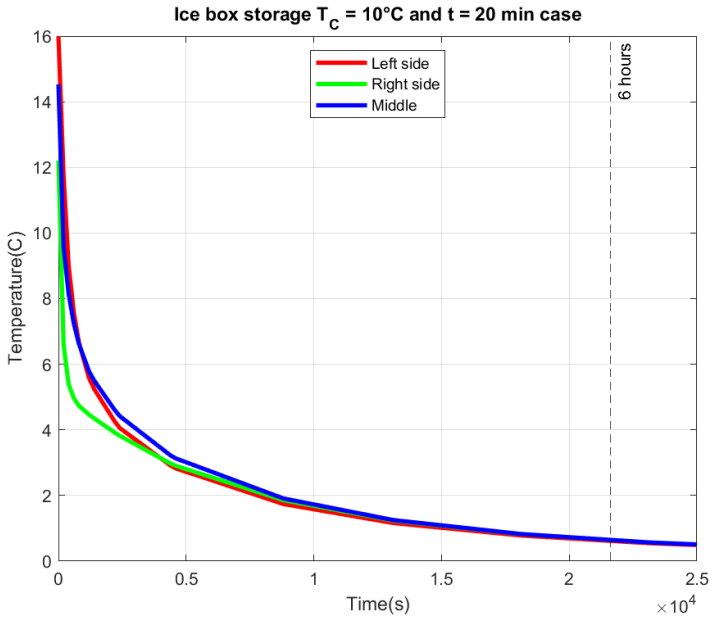

Figure 5.46: Ice box temperature plot for $T_C = 10^oC$ and second stage duration of 20 min.

Temperature plots show that during the icebox storage, the heart follows a significant cool-down process to the ice temperature. It shows that cooling down with ice at that temperature and filling the geometry until the level shown in Figure 5.40 affects the equilibrium temperature reached by the end of the storage process. In this case, assuming a cardioplegia temperature of $T_C = 1^oC$ and that it took $t = 10\,min$, it is possible to see that, on average, the heart reached an equilibrium temperature lower than temperatures that might affect the biological functions of the heart. Also, the equilibrium temperature obtained at the end of this second stage would be the initial condition for the next stage and it is a temperature greater than those temperatures reported to affect heart tissue performance. To compare the accuracy of the models performed, there was a validation case run using experimental conditions reported in literature [19]. This study reported that the evolution took place from temperatures in the range of $(6.1^oC - 6.2^oC)$ to temperatures near 0.3^oC after $t = 4h$ of exposure to ice [19]. Using those conditions and the temperature assumptions of the different

domains, it was possible to obtain the simulated curve shown in Figure 5.47. It is possible to see that it reaches temperatures in the range specified after $t = 4h$. The ice box dimensions matched experimental ice box measurements and the bag size used was the one used for the second stage. The temperatures shown below specify the simulated conditions used to perform the simulation.

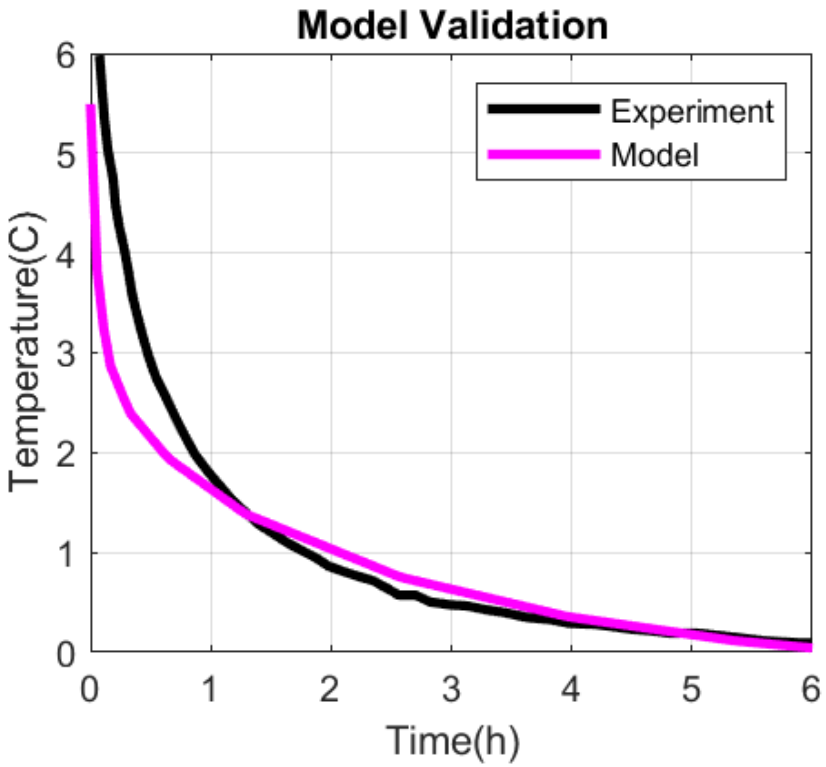

Figure 5.47: Validation case examined with experimental data reported in the literature. Simulated results were averaged between the three regions to approximate the temperature in comparison to the previous stages of processing data techniques. Simulated initial conditions matched experimental reported measurements [19].

5.3.3 Stage 4: Back-storage back table

The fourth stage of the process is removing the heart from the icebox and following a heat-up process due to the new bag in which the heart is being placed. On the other

hand, the ice level was reduced to the level of the second stage which means a lower level compared to the third stage. Moreover, the external heat transfer resistance condition is also included considering the exterior temperature. The saline solution and the bag dimensions assumptions explained in the second stage were also considered during the fourth stage. Figure 5.48 shows the geometry setup for the fourth stage. The case shown is the distribution temperature obtained for a cardioplegia that was performed in the first stage at $T_C = 1^oC$ and time of execution of t=10 min. The results shown as follows are the plots obtained from cardioplegia at $T_C = 1^oC$ and $t = 10\,min$ for the fourth stage. These plots shows that during the bag storage removal process, the heart follows a heat-up process due to the thermodynamic competition between the initial bag temperature and the equilibrium temperature reached in the previous stage. In other words, the heat-up process allows the heart to heat up in less than $10\,min$ to 9^oC on average. Also, the equilibrium temperature obtained at the end of this fourth stage would be the initial condition for the final stage of the process.

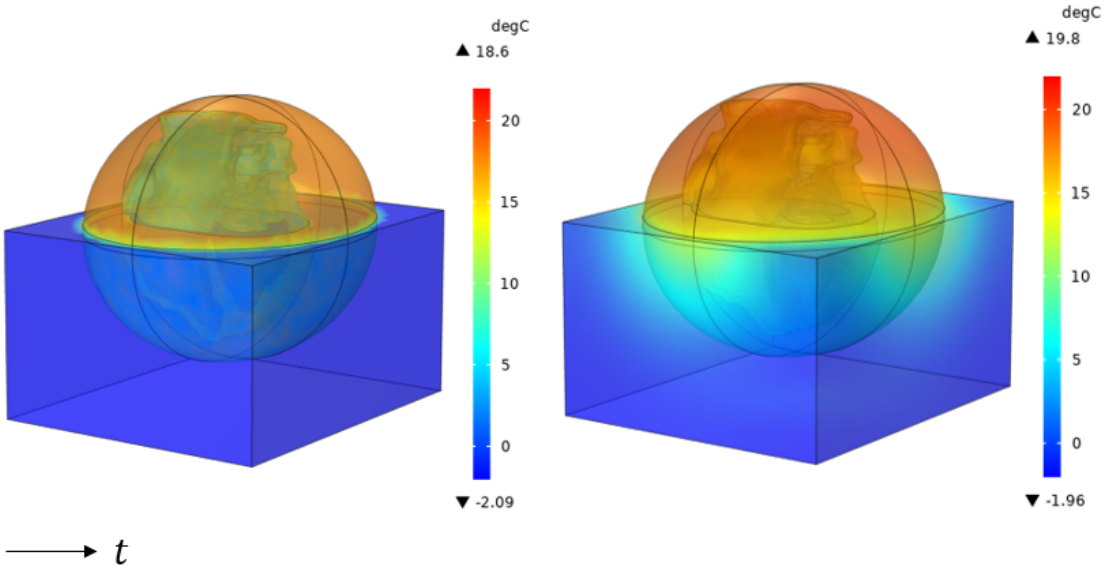

Figure 5.48: Back-table bag storage simulation for $T_C = 1^oC$ and $t = 10\,min$. The temperature distribution evaluates conduction and the external heat transfer resistance condition using the equilibrium temperatures from the previous stage. The first frame is for $t = 0\,min$ and $t = 10\,min$.

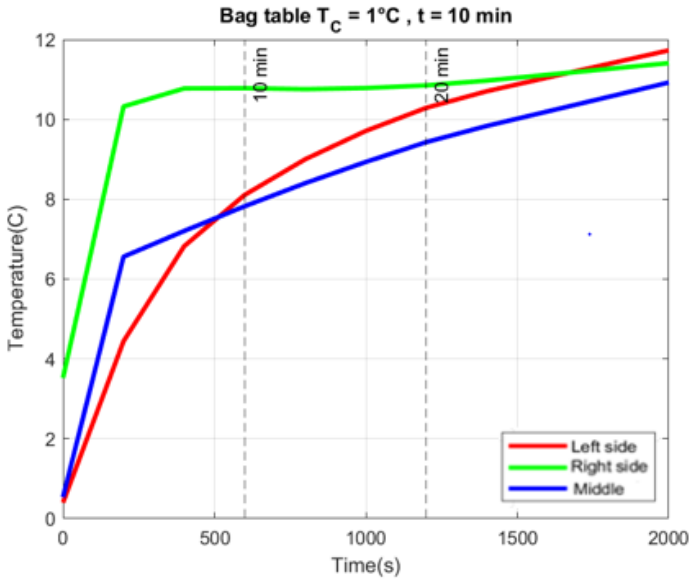

Figure 5.49: Back-table storage for $T_C = 1^oC$ and second stage execution time of $10\,min$.

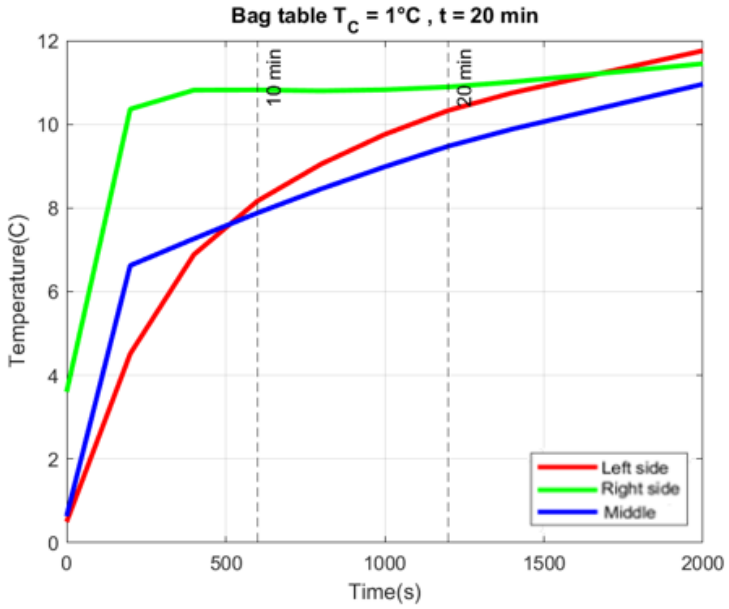

Figure 5.50: Back-table storage for $T_C = 1^oC$ and second stage execution time of 20 min.

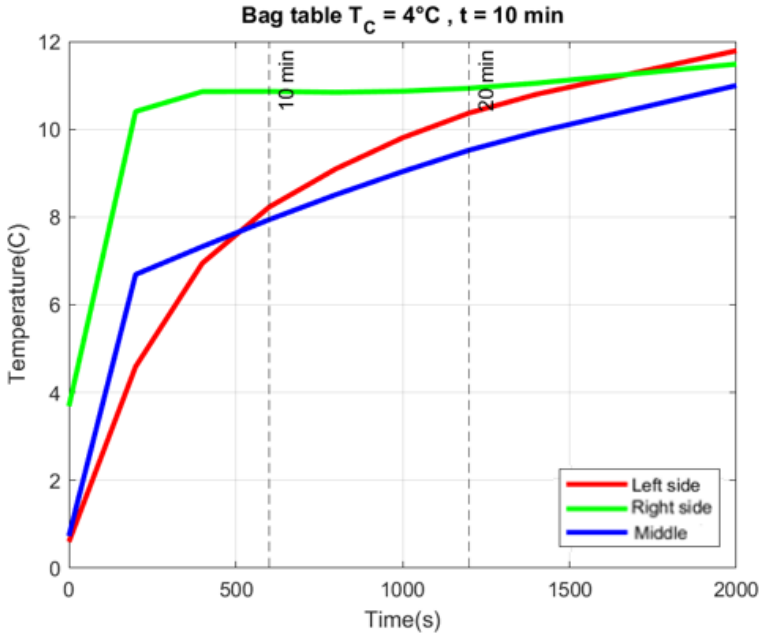

Figure 5.51: Back-table storage for $T_C = 4^oC$ and second stage execution time of 10 min.

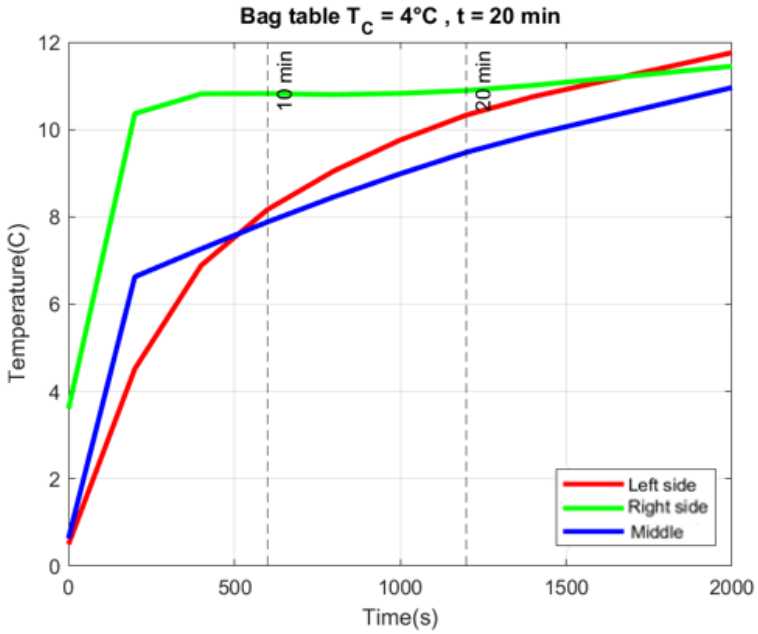

Figure 5.52: Back-table storage for $T_C = 4^oC$ and second stage execution time of 20 min.

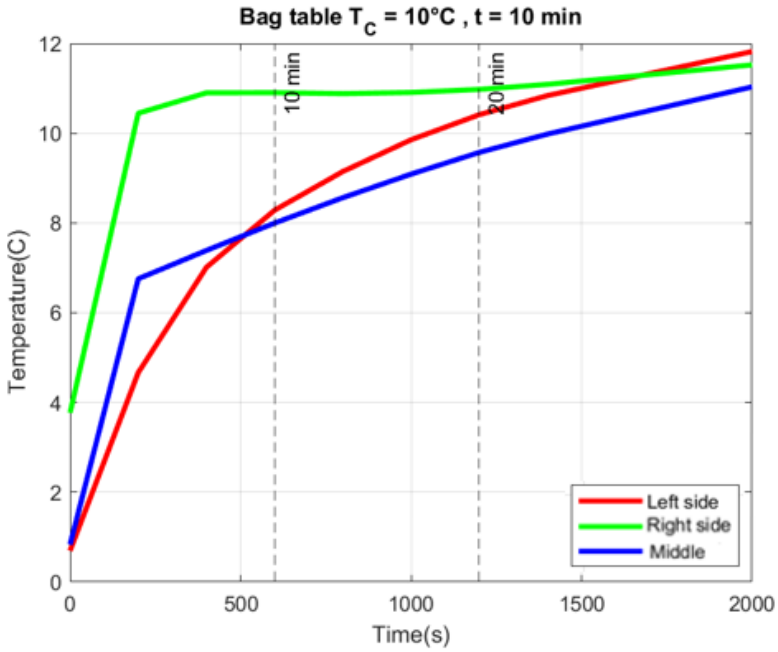

Figure 5.53: Back-table bag storage for $T_C = 10^oC$ and second stage execution time of 10 min.

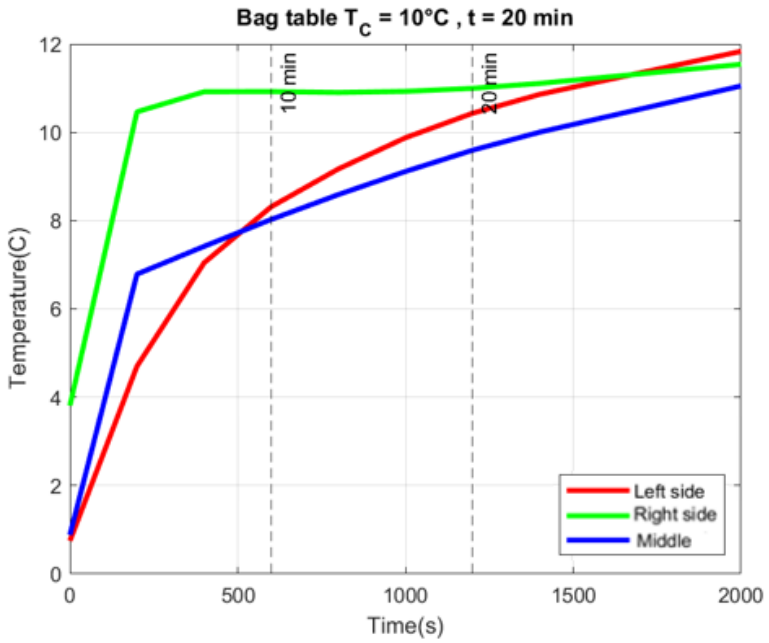

Figure 5.54: Back-table storage for $T_C = 10^oC$ and second stage execution time of 20 min.

5.3.4 Stage 5: Organ warm-up process

The fifth stage of the process is the final heat-up of the heart to body temperature. In this case, the simulation performed was set to see how long the heart takes to reach body temperature again from the equilibrium temperature reached at the end of the fourth stage. Figure 5.55 shows the geometry setup for the fifth stage. The case shown is the distribution temperature obtained for a cardioplegia that was performed in the first stage at $T_C = 1^oC$ and time of execution of t=10 min. Also, the following graphs show the temperature plots obtained for $T_C = 1^oC$ and $t = 10\,min$ specifically. As it was stated in the first stage simulation, the time that takes to perform the stage affects the equilibrium temperature reached at the end. Also, the different regions of the heart have differences in the temperature evolution.

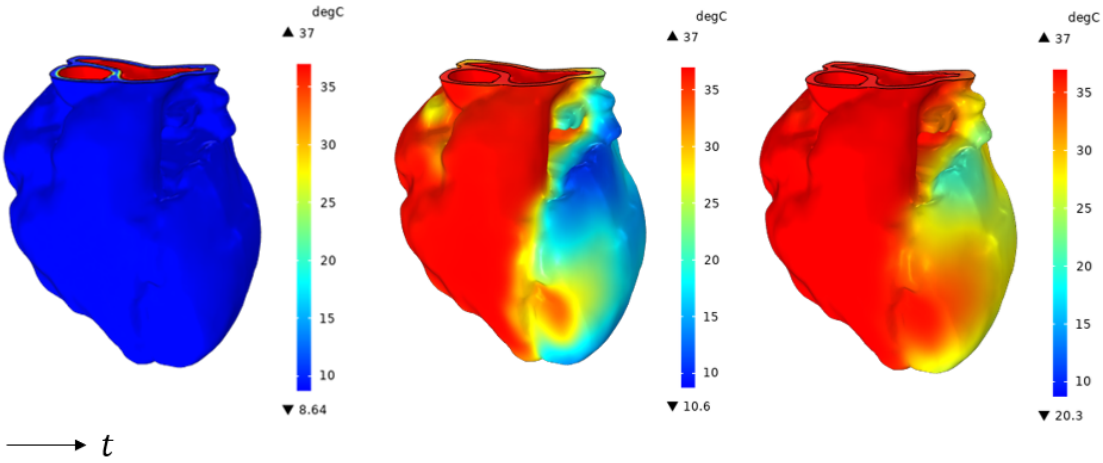

Figure 5.55: Heat-up surfaces for $T_C = 1^oC$ and $t = 10\,min$. The temperature distribution evaluates conduction heat transfer phenomena using the equilibrium temperatures from the previous stage. The first frame is for $t = 0\,min$. The second frame shows $t = 5\,min$ and the last frame shows $t = 10\,min$.

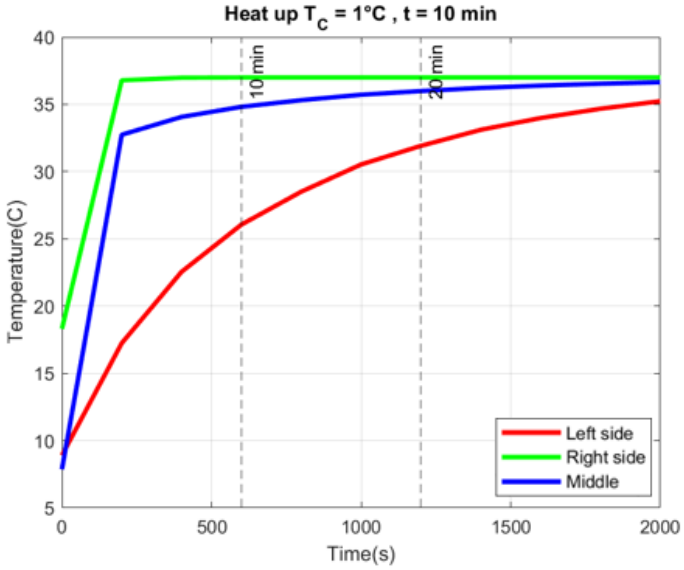

Figure 5.56: Warm-up temperature plots obtained for $T_C = 1^oC$ and a second stage execution time of $10\,min$.

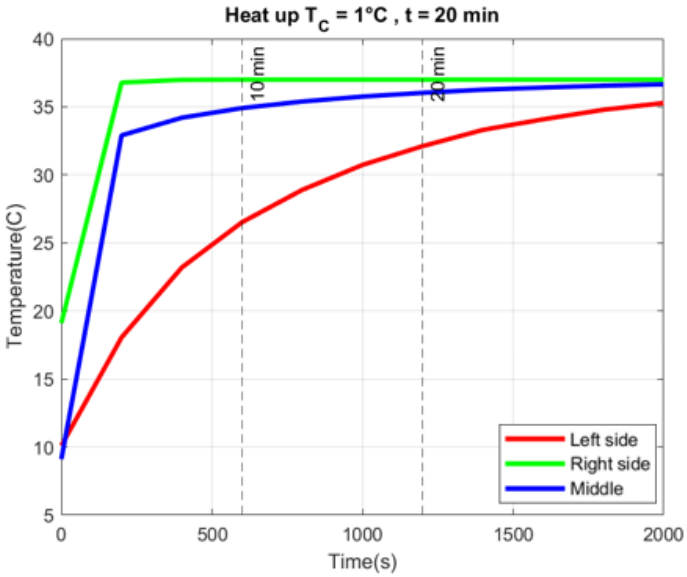

Figure 5.57: Warm-up temperature plots obtained for $T_C = 1^oC$ and a second stage execution time of 20 min.

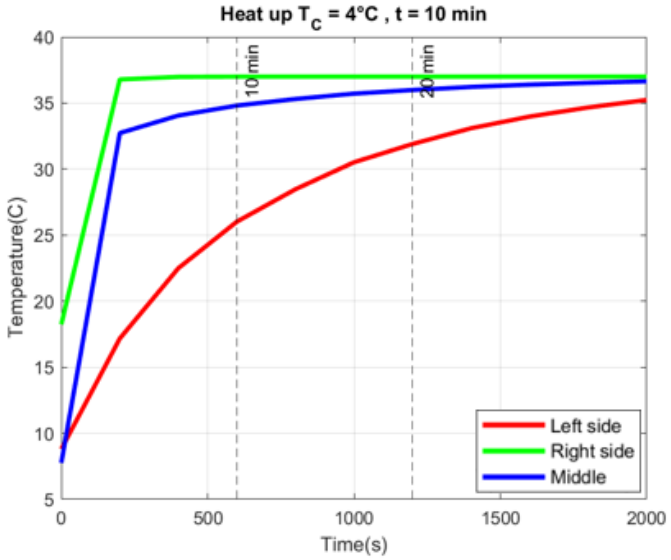

Figure 5.58: Warm-up temperature plots obtained for $T_C = 4^oC$ and a second stage execution time of 10 min.

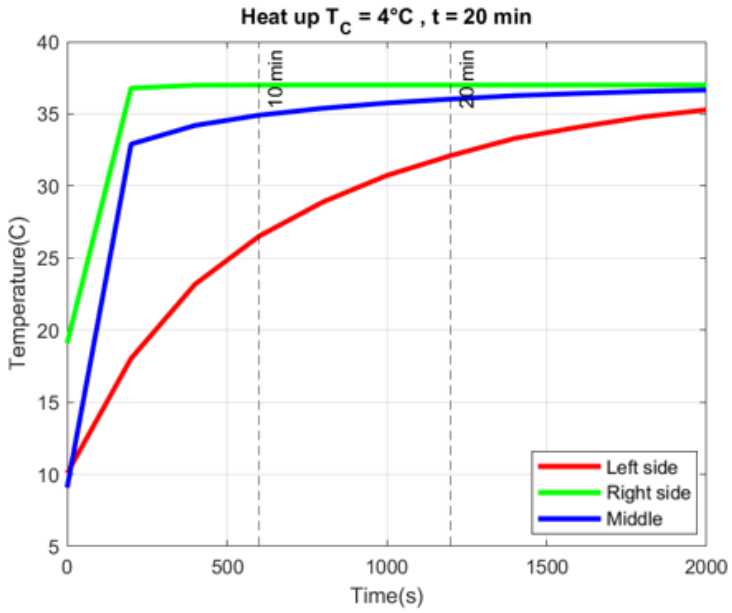

Figure 5.59: Warm-up temperature plots obtained for $T_C = 4^oC$ and a second stage execution time of 20 min.

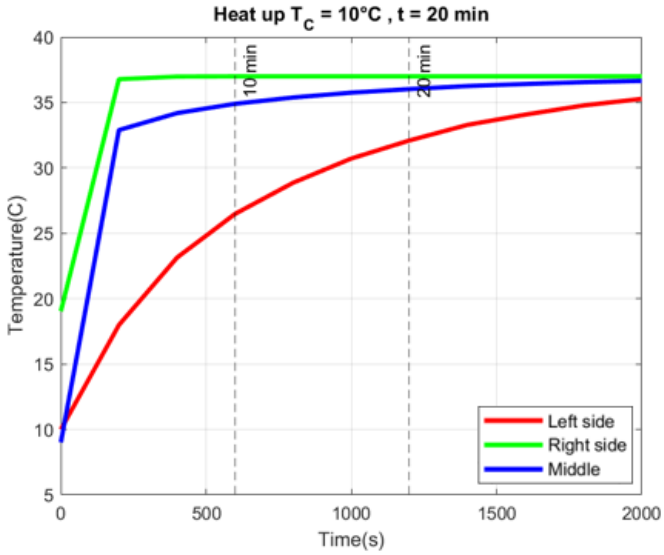

Figure 5.60: Warm-up temperature plots obtained for $T_C = 10^oC$ and a second stage execution time of 10 min.

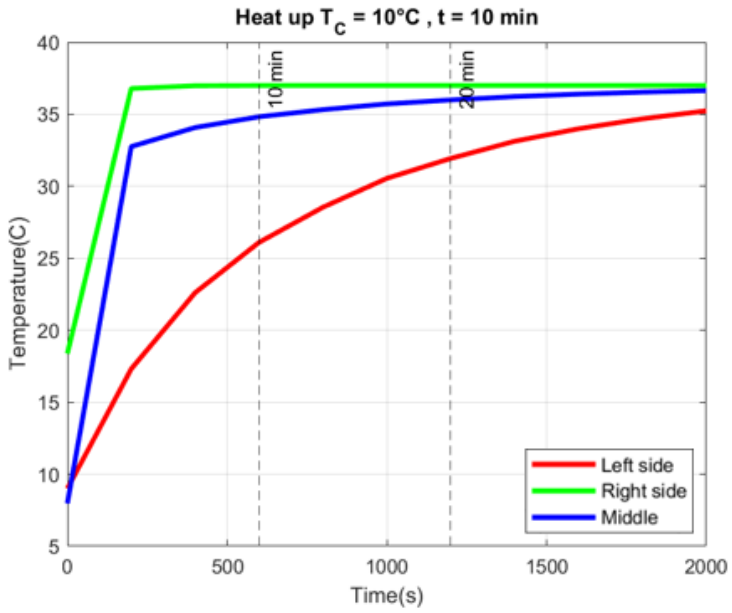

Figure 5.61: Warm-up temperature plots obtained for $T_C = 10^oC$ and a second stage execution time of 20 min.

5.4 Rates evolution

The cooling-down and warming-up rates were calculated to analyze how the heart temperature gradient changes through time. It is an important consideration for analyzing how fast temperature evolves and if this could affect the biological performance of the organ. Figure 5.62 shows the evolution of the gradient through time for different stages.

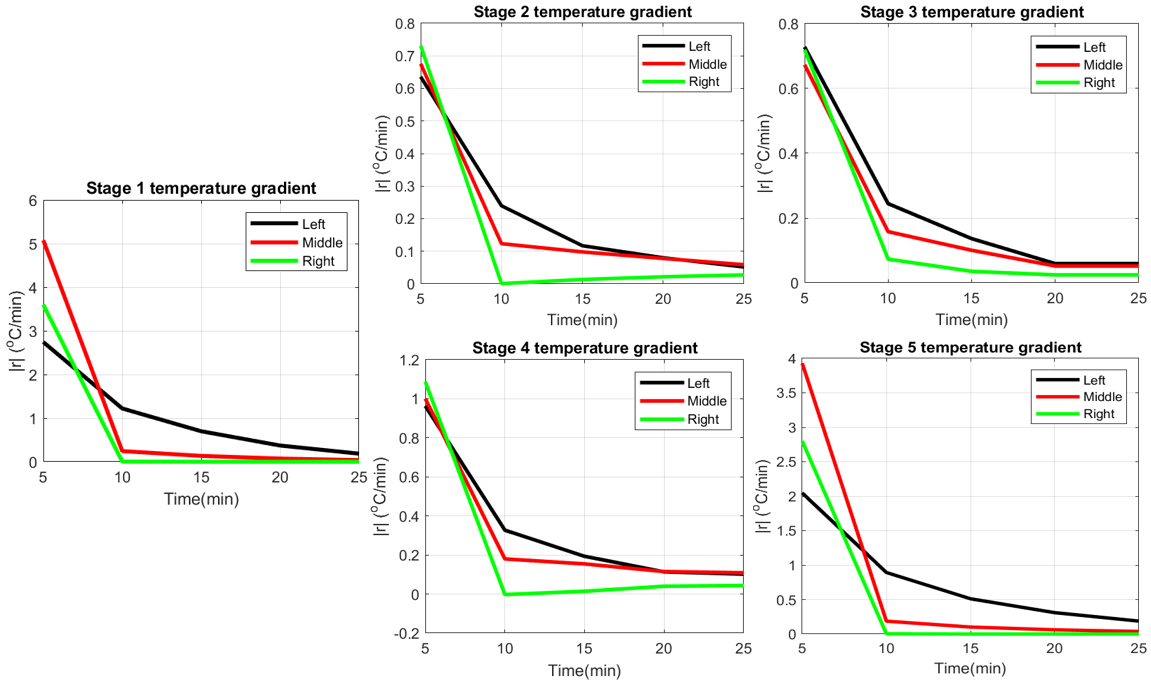

Figure 5.62: Temperature time gradient for the different stages.

Also, it is possible to plot the gradient evolution across stages for specific cases. Figure 5.63 shows the gradient time evolution when the cardioplegic solution is at $T_C = 1^oC$ and when the second stage takes $t = 10\,min$ to be done.

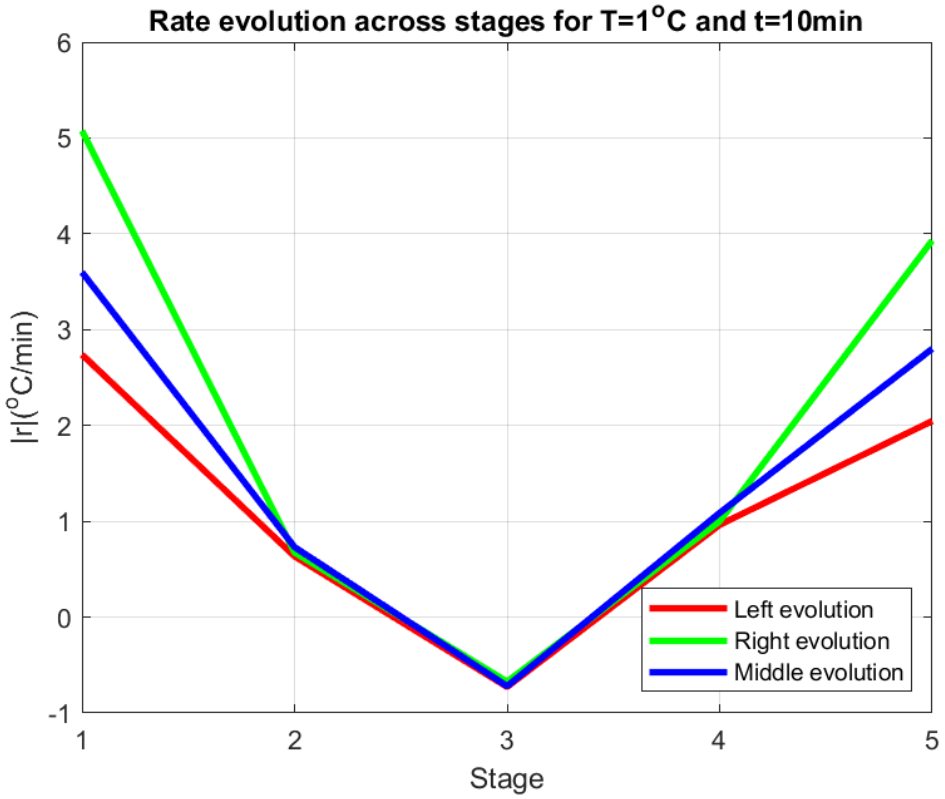

Figure 5.63: Rate evolution across all stages for the case of a cardioplegic solution performed at $T_C = 1^oC$ and a time of $t = 10\,min$. It is shown as absolute values to read the rate change.

Chapter 6

Discussion

Despite remaining the standard (or sometimes preferred) approach for heart transplants, and indeed for other organs, SCS has been linked to a higher risk of subsequent graft damage, cold injury, and protein denaturation. Upon declaration of death (either brain death or cardiac death) and deciding to proceed with heart transplants, the heart experiences a journey that exposes it to several temperature environments. Beginning (often) with hypothermic ischemia and administration of cold cardioplegia, the heart is cooled down, retrieved from the donor, placed in a cold storage container, and transported to the recipient. At the recipient location, the above processes are essentially reversed, from a thermal perspective, with warm ischemia until it is reconnected to the recipient's circulatory system. Indeed, warm ischemic time (WIT) is the single most critical parameter considered for assessing graft viability and is closely tracked to assess any evidence of IRI upon recipient cross-clamp release. At each of the above stages during the journey of the heart, the temperature, and indeed its distribution, within and throughout the organ is unknown. In this novel study, we demonstrated, for the first time, detailed 4D (3D+time) temperature distributions during each stage of the SCS heart transplant journey using state-of-the-art biothermal modeling on an

anatomically accurate heart model. Our results indicate that the thermal behavior of the organ (heart) is strongly dependent on initial conditions, boundary conditions surrounding the organ, and duration of exposure to these conditions.

In this study, multiple ranges of starting temperatures and times were explored. For the first stage S_1 – cardioplegia – the heart cools down in a matter of minutes but in a non-homogeneous manner. The temperature of the thinner regions of the heart (central-right regions) drops below 5^oC in less than 10 minutes for a cardioplegic solution at 1^oC. From there, the thinner regions could warm up to approximately 12^oC in 10 minutes during the back-table process (S_2) before placing it in the icebox. During the transportation of the heart on ice (S_3), the organ cools down and drops below 2^oC in approximately 30 minutes, following which it warms up (heterogeneously) to around 9^oC in approximately 10 minutes as it is prepped for implantation on the back table (S_4) at the recipient center. Finally, the heart warms up as it is placed within the body of the recipient (S_5), and the thinner regions can warm up very quickly to 35^oC in 10 minutes. The thicker regions, on the other hand, undergo a slower temperature change, lagging the thinner regions and taking more than twice as long to undergo similar temperature changes for each stage. Figure 6.1 shows how the temperature evolution across stages behaves for the particular case of a cardioplegic solution of $T = 1^oC$ and a second stage of $t = 10\,min$. On the other hand, figure 6.2 shows the normalized time evolution concerning the time of each stage. This allows us to see the evolution of temperature per stage.

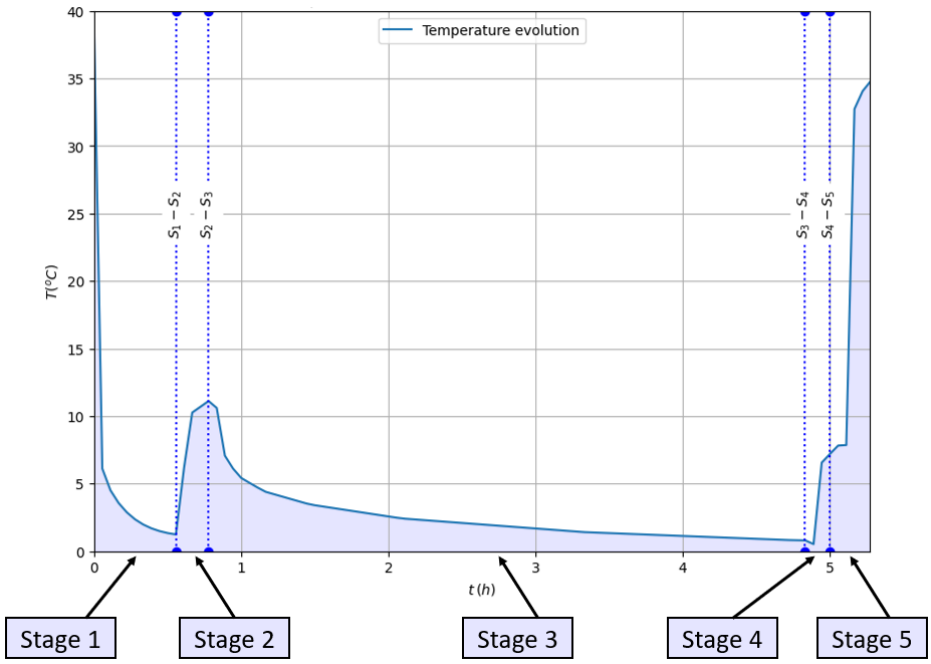

Figure 6.1: Stages temperature evolution across stages for a cardioplegic solution at $T_C = 1^oC$ and a second stage of $t = 10\,min$.

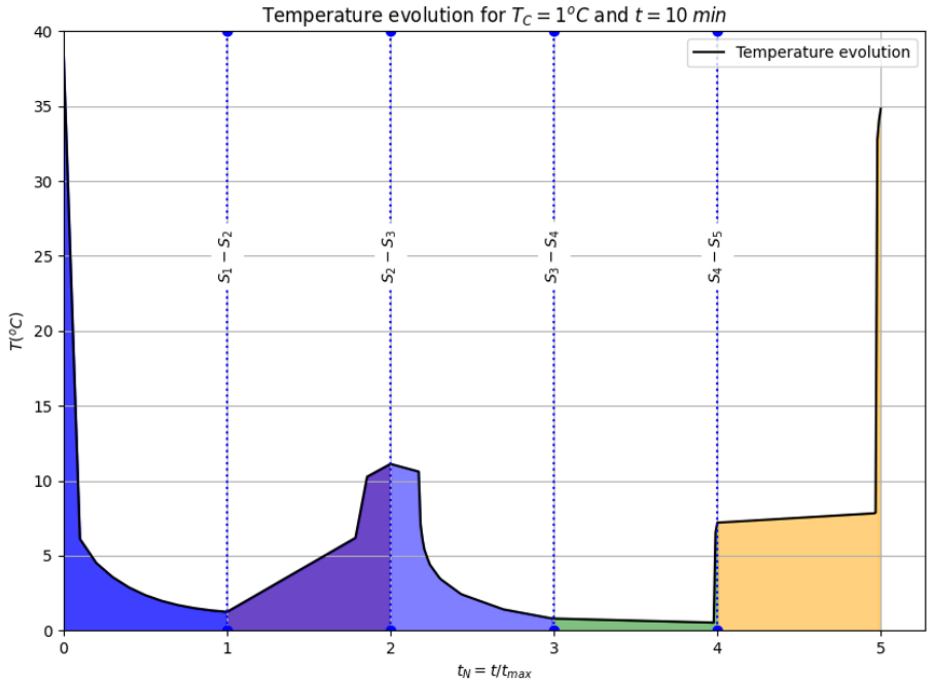

Figure 6.2: Normalized temperature evolution across stages for a cardioplegic solution at $T_C = 1^oC$ and a second stage of $t = 10\,min$.

It is also important to mention that the temperature changes are not uniform. Indeed, the temperature changes within the organ are significantly different and based on the thickness of the region. As mentioned above, the left side, which is thicker than the right, often takes twice as long to warm up and cool down during each stage. This is seen in temperature evolution figures, where there exists a gradient of temperature across the inner volume of the organ which persists for a considerable duration. For instance, during the first stage, the left heart is close to 14^oC at 10 minutes while the right and central regions are below 5^oC at the same instance of time. This heterogeneity between the left and right sides of the heart is just as stark during the final stage within the recipient's body, where the left side warms slowly, reaching a temperature of approximately 25^oC in 10 minutes, while the right side is approaching the body temperature of 37^oC at the same time instance. It is important to note that the starting temperature for all the cases studied was the same for all regions, thereby indicating the highly heterogeneous thermal behavior within the organ. Furthermore, some stages in the model do not account for an external heat transfer resistance as another stages do. This might result in possible changes in the values obtained for the cooling and heating rates.

This study has several implications for the current paradigm of SCS. It is believed that frostbite, cold injury, and protein denaturation may occur below 2^oC. In our study, the temperature of the heart drops below this threshold within 30 minutes when placed on ice. Other studies have reported that the average organ temperatures were measured to be below 2^oC after icebox transport, and below 0^oC after 6 hours as we see in our models as well. It is especially crucial to consider the heterogeneous temperature distribution within the organ at each stage of heart transplants. Further. as we determined in this study, different regions of the heart undergo a 'roller-coaster' experience

of thermal behavior and should be quantified to optimize this process. Recent advancements such as the introduction of preservation solution temperature monitoring in the Paragonix SherpaPak and/or normothermic perfusion such as the Transmedics OCS systems can help subject the organ to potentially more homogeneous and controlled temperatures. However, it is yet unclear what the ideal organ temperature should be. Furthermore, WIT and IRI are likely strongly associated with not only the average organ temperature but also the heterogeneous temperature distribution within the organ. Our study provides a platform to obtain high-fidelity temperature distributions within the organ subject to a plethora of real-life-mimicking situations, enabling quantifying and predicting the organ temperature for heart transplants. This is essential for not only optimizing current heart transplant strategies but for also expanding the donor pool.

Chapter 7

Final remarks

7.1 Conclusions

In this study, it was demonstrated, for the first time, detailed thermal responses and temperature distributions within the heart during each stage of heart transplants. Using an anatomically accurate cardiac geometry, we model the heat transfer through the organ using computational biothermal modeling. Results indicate that the heart experiences a roller-coaster-like temperature change during each stage including rapid cool down from body temperature of 37^oC to below 10^oC within 15 minutes in stage 1, followed by cool down and temperatures below 2^oC in the icebox during transport for a significant duration (more than 3 hours). As the heart reaches the recipient institution, the heart experiences a rapid warming-up approaching a body temperature of 37^oC in approximately 10 minutes. Interestingly, the temperature distribution throughout the heart at each stage is heterogeneous, with the right side experiencing rapid temperature changes at a rate often two times as fast as the left side due to varying thickness. The rapid temperature changes, extended duration of sub-2^oC during SCS transport, and heterogeneous temperature distributions throughout the heart at each stage of heart

transplants have implications for frostbite injury and organ viability, necessitating further in-depth studies.

7.2 Future Work

The future work of this study is based on the diversity of available organs because this study could allow potentially a patient-specific analysis for personalized modeling. This also means analyzing how the heat transfer affects different organs, shapes, sizes, and configurations depending on the particular case conditions. This study considered a normal physiological size heart assuming that it was only composed of heart muscle throughout the whole domain. The thermal properties were obtained from a publicly available database and may not accurately reflect the diversity in patient population, age, gender, and other factors. On the other hand, as it was mentioned, the material properties in this study were assumed not to have a temperature dependence which affects the results obtained in these initial simulations. The cardiac model was simplified to remove the valves, which may influence the temperature behavior because this means that additional materials other than heart muscle were not considered. The first stage of cardioplegic cooling assumed that the interior volume of the heart chambers was filled with the cooling solution for simplicity which can also influence the cooling rate. In these simulations, natural convection due to movement is not considered, which makes flow-dependent convection resistance negligible for these cases. On the other hand, the air layer located inside the ice box is small enough to not consider natural convection due to its presence. This means that the Reynolds number and the Nusselt number are not significant in considering that layer as a part of the model for these simulations. Additionally, the orientation of the organ could play an important role in how the heart is cooled down or affected by the temperature gradients present.

Future models will include more complexity based on the availability of high-fidelity data. This complexity will include convection due to fluid flow throughout the geometry such as blood flow or pumping the cardioplegic solution. Also, a more complex model might include the mass transfer effect that takes place in considering the heart materials as porous media. Additionally, COMSOL allows including a heat transfer module that considers chronic tissue damage using specified temperatures depending on the material evaluated.

Bibliography

[1] Abbas Ardehali, Fardad Esmailian, Mario Deng, Edward Soltesz, Eileen Hsich, Yoshifumi Naka, Donna Mancini, Margarita Camacho, Mark Zucker, Pascal Leprince, et al. Ex-vivo perfusion of donor hearts for human heart transplantation (proceed ii): a prospective, open-label, multicentre, randomised non-inferiority trial. *The Lancet*, 385(9987):2577–2584, 2015.

[2] Maria Irene Bellini and Vito D'Andrea. Organ preservation: which temperature for which organ?, 2019.

[3] R Byron Bird, Warren E Stewart, Edwin N Lightfoot, and Robert E Meredith. Transport phenomena. *Journal of The Electrochemical Society*, 108(3):78C, 1961.

[4] Macit Bitargil, Osama Haddad, Si M Pham, Neha Garg, Samuel Jacob, Magdy M El-Sayed Ahmed, Kevin Landolfo, Parag C Patel, Rohan M Goswami, Juan Carlos Leoni Moreno, et al. Packing the donor heart: Is sherpapak cold preservation technique safer compared to ice cold storage. *Clinical Transplantation*, 36(8):e14707, 2022.

[5] Macit Bitargil, Osama Haddad, Si M Pham, Rohan M Goswami, Parag C Patel, Samuel Jacob, Magdy M El-Sayed Ahmed, Juan Carlos Leoni Moreno, Daniel S Yip, Kevin Landolfo, et al. Controlled temperatures in cold preservation provides safe heart transplantation results. *Journal of Cardiac Surgery*, 37(4):732–738, 2022.

[6] Hong Chee Chew, Peter S Macdonald, and Kumud K Dhital. The donor heart and organ perfusion technology. *Journal of thoracic disease*, 11(Suppl 6):S938, 2019.

[7] AB Comsol. Heat transfer module user's guide comsol. *Inc., Burlington, MA*, 2006.

[8] Maria G Crespo-Leiro, Marco Metra, Lars H Lund, Davor Milicic, Maria Rosa Costanzo, Gerasimos Filippatos, Finn Gustafsson, Steven Tsui, Eduardo Barge-Caballero, Nicolaas De Jonge, et al. Advanced heart failure: a position statement of the heart failure association of the european society of cardiology. *European journal of heart failure*, 20(11):1505–1535, 2018.

[9] Jason F Goldberg, Lauren K Truby, Sean Agbor-Enoh, Annette M Jackson, Christopher R Defilippi, Kiran K Khush, and Palak Shah. Selection and interpretation of molecular diagnostics in heart transplantation. *Circulation*, 148(8):679–694, 2023.

[10] Federica Guidetti, Mattia Arrigo, Michelle Frank, Fran Mikulicic, Mateusz Sokolski, Raed Aser, Markus J Wilhelm, Andreas J Flammer, Frank Ruschitzka, and Stephan Winnik. Treatment of advanced heart failure—focus on transplantation and durable mechanical circulatory support: What does the future hold? *Heart Failure Clinics*, 17(4):697–708, 2021.

[11] Nicholas R Hess, Luke A Ziegler, and David J Kaczorowski. Heart donation and preservation: Historical perspectives, current technologies, and future directions. *Journal of Clinical Medicine*, 11(19):5762, 2022.

[12] Steven M Hollenberg, JoAnn Lindenfeld, Frederick A Masoudi, Patrick E McBride, Pamela N Peterson, Lynne Warner Stevenson, Cheryl Westlake, Sana M Al-Khatib, Biykem Bozkurt AACC, Joaquin E Cigarroa, et al. 2016 acc/aha/hfsa focused update on new pharmacological therapy for heart failure: an update of the 2013 accf/aha guideline for the management of heart failure. *Journal of Cardiac Failure*, 22(9), 2016.

[13] Valerie Kouskoff, Lin Yuan, Feng Yue, Jacek Z Kubiak, Sen Wu, Yongye Huang, Lin Yuan[1], Feng Yue, Sen Wu, and Yongye Huang. Open access edited and reviewed by. *Applying large animals for developmental study and disease modeling*, page 4, 2023.

[14] Sanne JJ Langmuur, Jorik H Amesz, Kevin M Veen, Ad JJC Bogers, Olivier C Manintveld, and Yannick JHJ Taverne. Normothermic ex situ heart perfusion with the organ care system for cardiac transplantation: a meta-analysis. *Transplantation*, 106(9):1745–1753, 2022.

[15] F Latif, G Sayer, D Lotan, J Mendoza, M Regan, D Tsapepas, A Ramakrishnan, EM DeFilippis, M Yuzefpolskaya, P Colombo, et al. The effect of temperature control versus icebox preservation on post heart transplant outcome. *The Journal of Heart and Lung Transplantation*, 42(4):S221, 2023.

[16] Silvana F Marasco, Ashley Kras, Elliot Schulberg, Matthew Vale, and GA Lee. Impact of warm ischemia time on survival after heart transplantation. In *Transplantation proceedings*, volume 44, pages 1385–1389. Elsevier, 2012.

[17] Gérard A Maugin. *The thermomechanics of nonlinear irreversible behaviours*, volume 27. World scientific, 1999.

[18] SG Michel, GM LaMuraglia Ii, MLL Madariaga, and Lisa M Anderson. Innovative cold storage of donor organs using the paragonix sherpa pak™ devices. *Heart, lung and vessels*, 7(3):246, 2015.

[19] P Patel, B Bulka, L Churchill, M Tajima, and L Anderson. Ice is not 4c: Thermodynamic characterization of lungs and hearts preserved on ice. *The Journal of Heart and Lung Transplantation*, 42(4):S122–S123, 2023.

[20] Guangqi Qin, Yang Su, Trygve Sjöberg, and Stig Steen. Oxygen consumption of the aerobically-perfused cardioplegic donor heart at different temperatures. *Annals of Transplantation*, 23:268, 2018.

[21] Dejan Radakovic, Seymur Karimli, Kiril Penov, Ina Schade, Khaled Hamouda, Constanze Bening, Rainer G Leyh, and Ivan Aleksic. First clinical experience with the novel cold storage sherpapak™ system for donor heart transportation. *Journal of Thoracic Disease*, 12(12):7227, 2020.

[22] Martin O Schmiady, Tim Graf, Ahmed Ouda, Raed Aser, Andreas J Flammer, Paul R Vogt, and Markus J Wilhelm. An innovative cold storage system for donor heart transportation—lessons learned from the first experience in switzerland. *Journal of Thoracic Disease*, 13(12):6790, 2021.

[23] Jacob N Schroder, Chetan B Patel, Adam D DeVore, Benjamin S Bryner, Sarah Casalinova, Ashish Shah, Jason W Smith, Amy G Fiedler, Mani Daneshmand, Scott Silvestry, et al. Transplantation outcomes with donor hearts after circulatory death. *New England Journal of Medicine*, 388(23):2121–2131, 2023.

[24] Angela Felicia Sunjaya, Anthony Paulo Sunjaya, et al. Combating donor organ shortage: organ care system prolonging organ storage time and improving the outcome of heart transplantations. *Cardiovascular therapeutics*, 2019, 2019.

[25] Lu Wang, Guy A MacGowan, Simi Ali, and John H Dark. Ex situ heart perfusion: The past, the present, and the future. *The Journal of Heart and Lung Transplantation*, 40(1):69–86, 2021.

[26] Clyde W Yancy, Mariell Jessup, Biykem Bozkurt, Javed Butler, Donald E Casey, Monica M Colvin, Mark H Drazner, Gerasimos Filippatos, Gregg C Fonarow, Michael M Givertz, et al. 2016 acc/aha/hfsa focused update on new pharmacological therapy for heart failure: an update of the 2013 accf/aha guideline for the management of heart failure: a report of the american college of cardiology/american heart association task force on clinical practice guidelines and the heart failure society of america. *Journal of the American College of Cardiology*, 68(13):1476–1488, 2016.

[27] Clyde W Yancy, Mariell Jessup, Biykem Bozkurt, Javed Butler, Donald E Casey Jr, Monica M Colvin, Mark H Drazner, Gerasimos S Filippatos, Gregg C Fonarow, Michael M Givertz, et al. 2017 acc/aha/hfsa focused update of the 2013 accf/aha guideline for the management of heart failure: a report of the american college of cardiology/american heart association task force on clinical practice guidelines and the heart failure society of america. *Circulation*, 136(6):e137–e161, 2017.

[28] Tingyang Zhou, Evan R Prather, Davis E Garrison, and Li Zuo. Interplay between ros and antioxidants during ischemia-reperfusion injuries in cardiac and skeletal muscle. *International journal of molecular sciences*, 19(2):417, 2018.